

# Influence of initial soil moisture in a Regional Climate Model study over West Africa. Part 1: Impact on the climate mean

Brahima KONÉ<sup>1</sup>, Arona DIEDHIOU<sup>1, 2</sup>, Adama Diawara<sup>1</sup>, Sandrine Anquetin<sup>2</sup>, N'datchoh Evelyne Touré<sup>1</sup>, Adama Bamba<sup>1</sup>, and Arsene Toka Koba<sup>1</sup>

<sup>1</sup>LASMES - African Centre of Excellence on Climate Change, Biodiversity and Sustainable Agriculture (ACE CCBAD) / Université Félix Houphouët Boigny, Abidjan, Côte d'Ivoire

<sup>2</sup>Univ. Grenoble Alpes, IRD, CNRS, Grenoble INP, IGE, F-38000 Grenoble, France

*Correspondence to:* Arona DIEDHIOU (arona.diedhiou@ird.fr)

## **Abstract.**

The impact of soil moisture initial conditions on the mean climate over West Africa was examined using the latest version of the Regional Climate Model of the International Centre for Theoretical Physics (RegCM4) at a horizontal resolution of 25 km × 25 km. The soil moisture reanalysis of the European Centre Meteorological Weather Forecast's reanalysis of the 20th century ERA20C is used to initialize the control experiment, while its minimum and maximum values over the entire domain are used to establish the initial dry and wet soil moisture conditions respectively (hereafter dry and wet experiments). For the control, the wet and dry experiments, an ensemble of five runs from June to September are performed. In each experiment, we analyzed the two idealized simulations most sensitive to the dry and wet soil moisture initial conditions. The impact of soil moisture initial conditions on precipitation in West Africa is linear over the Central and West Sahel where dry (wet) experiments lead to rainfall decrease (increase). The strongest precipitation increase is found over the West Sahel for wet experiments with a maximum change value of approximately 40%, while the strongest precipitation decrease is found for dry experiments over Central Sahel with a peak of change of approximately -4%. The sensitivity of soil moisture initial condition can persist for three to four months (90-120 days) depending on the region. However, the influence on precipitation is no longer than one month (between 15 and 30 days). The strongest temperature decrease is located over the Central and West Sahel with a maximum change of approximately -1.5 °C in wet experiments, while the strongest temperature increase is found over the Guinea Coast and Central Sahel for the dry experiments, with a maximum of change around 0.6°C. A significant

impact of soil moisture initial conditions on the surface energy fluxes is noted: in the wet (dry) experiments, a cooling (warming) of surface temperature is associated with a decrease (increase) of sensible heat flux, an increase (decrease) of latent heat flux and a decrease (increase) of the boundary layer depth. Part II of this study investigates the influence of soil moisture initial conditions on climate extremes.

## 1 Introduction

In the climate system, soil moisture is a crucial variable that **influences** water balance and surface energy components through latent surface fluxes and evaporation. Therefore, soil moisture impacts the development of weather patterns and precipitation. The strength of soil moisture impacts on land-atmosphere coupling varies with location and season. Koster et al. (2004) sustained that improving the simulation of the atmospheric response to the slow variations of land and ocean surface conditions may be important for seasonal climate prediction. The atmospheric response to ocean temperature anomalies has been well documented (Kirtman et al. 1998; Rasmusson et al. 1982). Schär et al. 1999 sustained that the role of soils may be comparable to that of the oceans. The solar energy received by the oceans is stored in summer and used to heat the atmosphere in winter. Conversely, the precipitation received by the soil is stored in winter and the moistening (cooling) is returned to the atmosphere in summer. Through its impact on surface energy fluxes and evaporation, there are many additional impacts on the climate process of soil moisture, such as boundary-layer stability and air temperature (Hong and Pan, 2000; Kim and Hong 2006). Several studies have shown that the anomalies of soil moisture may persist for several weeks or months, however, its impact remains only for a shorter time in the atmosphere, not exceeding few days (Vinnikov and Yeserkepova 1991; Liu et al., 2014). **The important role of anomalies in soil moisture in the coupling between land and atmosphere has been shown in several studies, using numerical climate models (Zhang et al., 2011) and observation datasets (Zhang et al., 2008a; Dirmeyer et al., 2006). For instance, over East Asia, Zhang et al., (2011) showed that soil moisture is found to have a much stronger impact on daily maximum temperature variability than on daily mean temperature variability, but generally has small effects on daily minimum temperature, except in the eastern Tibetan Plateau. They showed that soil moisture has a prominent contribution to precipitation variability in many parts of western China.**

West Africa is known to exhibit strong coupling between soil moisture and precipitation (Koster et al., 2004). Several previous studies have been conducted over West Africa on a global scale

using atmospheric general circulation model (AGCMs) to investigate the impact of soil moisture initial conditions on the land-atmosphere coupling (Koster et al., 2004; Douville and al, 2001; Zhang et al., 2008b). However, at local and regional scales, the land-atmosphere coupling studies with AGCMs, present significant uncertainties (Xue et al. 2010). The regional climate models (RCMs) have been used to simulate the impact on interannual climate variability of anomalies in soil moisture (Seneviratne et al. 2006; Zhang et al. 2011). These studies have received a lot of attention due to the increase of climate variability associated with extreme weather events that have greater societal and environmental impacts. In general, these studies have been conducted in Asia, Europe and America (e.g. Seneviratne et al. 2006 for Europe; Zhang et al. 2011 for Asia; Zhang et al. 2008b for America). Overall, the results of these studies showed that during summer, the strong impact of the anomalies of soil moisture in land-atmosphere occurred mainly over the transition zones with a climate between wet and dry regimes, in agreement with Koster et al. (2004). The relevance and extent of this potential feedback are still poorly understood in West Africa.

This study will focus on the influence of soil moisture initial conditions on climate mean. It is based on performance assessment of the Regional Climate model version 4 coupled to the version 4.5 of the Community Land Model (RegCM4-CLM4.5) performed by Koné et al. (2018) where the ability of the model to reproduce the climate mean has been validated. The descriptions of the model and experimental setup used in this study are presented in Section. 2; in the Section 3, the influence of wet and dry soil moisture initial conditions on the subsequent climate mean is analyzed and discussed; and in Section 4 the main conclusions are presented. While this Part I investigates the impacts on the climate mean, the Part II of this article will be focused on the influence of soil moisture initial conditions on climate extremes.

## **2. Model and experimental design**

### **2.1 Model description and observed datasets**

The fourth generation of the Regional Climate Model (RegCM4) of the International Centre for Theoretical Physics (ICTP) is used in this study. Since its release, its physical representations have been continuously developed and implemented. The version used in the present study is RegCM4.7. The MM5 (Grell et al., 1994) non-hydrostatic dynamical core has been ported to RegCM without removing the existing hydrostatic core. The model dynamical core used in this study is non-hydrostatic. RegCM4 is a limited area model using a sigma pressure vertical grid and the finite differencing algorithm of Arakawa B-grid (Giorgi et al., 2012). The radiation scheme used in this version of RegCM4.7 is derived from the National Center for Atmospheric

Research (NCAR) Community Climate Model Version three (CCM3) (Kiehl et al., 1996). Aerosols representation is from Zakey et al. (2006) and Solomon et al. (2006). The large-scale precipitation scheme is from Pal et al. (2000) and the moisture scheme is the SUBgrid EXplicit moisture scheme (SUBEX). The SUBEX take into account the sub-grid scale cloud variability, and the accretion processes and evaporation for stable precipitation following the work of Sundqvist et al., 1989. In the planetary boundary layer (PBL), the sensible heat over ocean and land, water vapour and turbulent transport of momentum are calculated according to the scheme of Holtslag et al. (1990). Heat and moisture, the momentum fluxes of ocean surfaces in this study are computed as in Zeng et al. (1998). In RegCM4.7, convective precipitation and land surface processes can be described by several parameterizations. Based on Koné et al. (2018), we selected the convective scheme reported by Emanuel (1991) and the interaction processes between soil, vegetation and atmosphere are parameterized with CLM4.5. In each grid cell, CLM4.5 has 16 different Plant Functional Types (PFTs) and 10 soil layers (Lawrence et al., 2011; Wang et al., 2016). RegCM4 is integrated over the domain of West Africa depicted in Fig. 1 with 25 km (182x114 grid points; from 20° W-20° E and 5° S-21° N) with horizontal resolution and with 18 vertical levels and the initial and boundary conditions are taken from the European Centre for Medium-Range Weather Forecasts reanalysis (EIN75; Uppala et al., 2008; Simmons et al., 2007). The sea surface temperatures are obtained from the National Oceanic and Atmosphere Administration (NOAA) optimal interpolation weekly (OI\_WK) (Reynolds et al., 1996). The topography data are taken from the States Geological Survey (USGS) Global Multi-resolution Terrain Elevation Data (GMTED; Danielson et al., 2011) at 30 arc-second spatial resolution, which is an update to the Global Land Cover Characterization (GTOPO; Loveland et al., 2000) dataset.

Our analysis focuses on precipitation and the 2 m air temperature over the West African domain during the June-July-August-September (JJAS). We validate the simulated precipitation with the dataset from the Climate Hazards Group Infrared Precipitation with Stations (CHIRPS) developed at the University of California at Santa Barbara at the 0.05° high-resolution available from 1981 to 2020 (Funk et al., 2015). The validation of the simulated 2 m temperature relies on the CRU datasets (Climate Research Unit version 3.20) from the University of East Anglia, gridded at a horizontal resolution of 0.5° for 1901 to 2011 (Harris et al., 2013). To facilitate comparison between RegCM4 simulations, all products has been re-gridded to  $0.22^{\circ} \times 0.22^{\circ}$  using a bilinear interpolation method (Nikulin et al., 2012).

## 2.2 Experiments setup and analysis methodology

The European 20th Century Weather Prediction Center ERA20C soil moisture reanalysis is used to initialize the control experiment, while its domain-wide minimum and maximum values are used to establish the initial dry and wet soil moisture conditions respectively (hereafter dry and wet experiments). We initialized the dry and wet soil moisture initial conditions (in volumetric fraction  $\text{m}^3.\text{m}^{-3}$ ) respectively at the minimum value ( $=0.117*10^{-4}$ ) and the maximum value ( $=0.489$ ).

We designed three experiments (reference, wet, and dry), each with an ensemble of five (5) simulations starting from June 1st to September 30th. The difference between these three experiments is the change in the initial soil moisture condition (reference initial soil moisture condition, wet initial soil moisture condition, and dry initial soil moisture condition) during the first day of the simulation (June 1<sup>st</sup> 2001, 2002, 2003, 2004 and 2005) over the West African domain. Then, we selected the two runs most impacted by the wet and dry soil moisture initial conditions in order to exhibit the effects on the climate mean beyond the limits of the impacts of RegCM4 initial soil moisture internal forcing. In the same context, several previous studies have selected two extreme years to investigate the climate models sensitivity to soil moisture initial conditions (Hong et al., 2000; Kim and Hong, 2006) outside Africa.

Hong and al. (2000) used only two years (three months per year) to investigate the impact of initial soil moisture over North America (in the Great Plains) during two summers spanning May-June-July (MJJ) in 1988 (corresponding to a drought) and 1993 (corresponding to a flooding event). Kim and Hong (2006) selected two contrasting years 1997 (below normal precipitation) and 1998 (above normal precipitation year) for their study over east Asia. The first seven days (Kang et al., 2014) are excluded from the analysis as a spin-up period. Except the geographical location, the experimental setup is the same as that of Hong and Pan (2000). The geographical location of this study is the same as in Koné et al. (2018), with four sub-regions (Fig. 1) exhibiting different features of the annual precipitation cycle: Central Sahel ( $10^{\circ}$  W -  $10^{\circ}$  E;  $10^{\circ}$  N -  $16^{\circ}$  N), West Sahel ( $18^{\circ}$  W -  $10^{\circ}$  W,  $10^{\circ}$  N -  $16^{\circ}$  N), and Guinea Coast ( $15^{\circ}$  W -  $10^{\circ}$  E;  $3^{\circ}$  N -  $10^{\circ}$  N).

In several previous studies (Liu et al., 2014; Hong and Pan, 2000; Kim and Hong, 2006), the mean biases (MB) averaged over their studied domains are used to quantify the impact of the soil moisture initial conditions. In our study, we used the MB and the probability density function (PDF; Gao et al., 2016; Jaeger and Seneviratne, 2011) by fitting a normal distribution to better capture how many grid points are impacted by soil moisture initial conditions. The pattern correlation coefficient (PCC) is also used as a spatial correlation to reveal the degree of large-scale similarity between model simulations and observations. These performance metrics (MB,

PCC, and PDF) are computed for both modeled and observed temperature and precipitation only over land grid points.

For the two years most sensitive to soil moisture initial conditions, the Student t-test is used to compare the significance of the difference between a wet or dry sensitivity test (sample 1) and the control (sample 2) in assuming that our two samples are independent and in considering that this method performs well for climate simulations compared to more sophisticated techniques developed to address autocorrelation (Damien et al., 2014). The Student t-test is extensively used for analysis in climate sciences; it is fairly robust and easy to use and interpret (Menedez et al., 2019; Talahashi and Polcher, 2019). The Student t-test takes into account, the difference between the means of each sample, the variance (S) and the number of degrees of freedom ( $n - 1$ ), which depends on the sample size (n). The test statistic is calculated as:

$$t = \frac{\bar{X}_1 - \bar{X}_2}{\sqrt{\frac{S_1^2}{n_1} + \frac{S_2^2}{n_2}}}$$

Where  $\bar{X}_1$  ( $\bar{X}_2$ ) are the sample means,  $n_1$  ( $n_2$ ) are the sample sizes and  $S_1^2$  ( $S_2^2$ ) are the sample variances. In this study, the t-test at the 95% confidence level is used to consider statistically significant.

### 3. Results and discussion

#### 3.1. Influence of soil moisture initial conditions on precipitation.

To identify the two runs most impacted by the dry and wet experiments among the ensemble of five simulations (initiated on 1<sup>st</sup> June 2001, 2002, 2003, 2004 and 2005), we superimposed on Figure 2, the magnitude of daily soil moisture changes of the 5 runs compared to their corresponding control experiment over West African domain. Figure 2 shows that for the dry experiments (negative values of daily soil moisture changes), the weakest and strongest impacts of soil moisture initial conditions are found with the runs initiated on 1<sup>st</sup> June 2004 and 2003 respectively. For the wet experiments (positive values of daily soil moisture changes), the weakest impact is found for the run initiated on 1<sup>st</sup> June 2003, while the other runs exhibit quite the same strong sensitivity. From these results, we selected the two runs initiated on June 1<sup>st</sup>, 2003 and June 1<sup>st</sup>, 2004 as the simulations most influenced by the initial wet and dry soil moisture conditions, respectively, to better highlight the effects on the climate mean beyond the limits of the impact of the initial internal soil moisture forcing. It is worth noting that 2003 is



wetter than 2004 and is more sensitive to the dry experiment. While 2004 which is drier than 2003 is more sensitive to the wet experiment.

Figure 3 displays the spatial distribution of the observed mean rainfall (mm/day) from CHIRPS (Fig. 3a, c) for the runs JJAS 2003 and JJAS 2004 and the simulated from control experiments (Fig. 3b, d) initialized with reanalysis soil moisture ERA20C. Table 1 reports the MB and PCC for model simulation compared to CHIRPS, computed for the Central Sahel, Guinea Coast, West Sahel, and the entire West African domain. The CHIRPS product displays a zonal band of rainfall centered around 10° N, decreasing from North to South (Fig. 3a, c). The maximum values are located over the mountain regions of Cameroun and Guinea. While the precipitation minimum values are found over the Sahel and the Sahara. The control experiments (Fig. 3 b and d) reproduced the large-scale pattern of observed rainfall with PCC = 0.72 and 0.77 for the runs JJAS 2003 and JJAS 2004, respectively (Table 1). The spatial extent of rainfall maxima and the North-South gradient are well captured by control experiments; however, their magnitudes are underestimated with respect to the CHIRPS observation. Over West African domain, dry MB reaching -49.31% and -50.56% are obtained for the runs JJAS 2003 and JJAS 2004, respectively (Table 1). Fig. 4 displays the change in mean precipitation (in %) in JJAS 2003 and JJAS 2004 for dry and wet experiments with respect to the control experiments. The dotted area shows changes with a statistical significance of 95%.

Dry and wet sensitivity experiments showed that precipitation is significantly affected by soil moisture initial conditions at magnitude varying with the sub-regions (Fig. 4). Over the Central Sahel, for the dry experiments (Fig. 4a, c), we found a precipitation decrease for JJAS 2003 and JJAS 2004 (Fig. 4a, c). On the other hand, over the Guinea coast, we found an increase in rainfall for both JJAS 2003 and JJAS 2004. For the wet experiments (Fig. 4b, d), there is an increase of rainfall over most of studied domains studied for both JJAS 2003 and JJAS 2004. Overall, the impact of the soil moisture initial conditions on the precipitation is linear only over the Central Sahel for both JJAS 2003 and 2004. Therefore, the dry (wet) experiments exhibits significant decrease (increase) in precipitations with respect to the control experiments (Fig. 4a, c).

For a better quantitative evaluation, the PDF distributions of precipitation changes in JJAS 2003 and JJAS 2004, over (a) central Sahel, (b) west Sahel, (c) Guinea coast and (d) West Africa obtained from dry and wet experiments with respect to the control experiments are shown in Fig. 5. Table 2 summarizes the maximum values of changes obtained from the PDF's of the different

variables used in this study. The impact on precipitation of the soil moisture initial conditions is linear only over Central Sahel (Fig.5a) where the change in dry (wet) experiments showed a precipitation decrease (increase). The strongest precipitation increase is found over West Sahel for the wet experience with maximum change reached 40%. However, the strongest precipitation decrease is found over the Central Sahel for dry experiment with a maximum change value about -4% (Table 2). We noted that the impacts on precipitation of the wet experiments are greater than those from dry experiments (Table 2). These results are consistent with previous studies that supported a strong relationship between precipitation and soil moisture in particular over the transition zones with a climate between wet and dry climate regimes (Koster et al., 2004; Liu et al., 2014; Douville et al., 2001).

Fig. 6 and Fig. 7 shows the changes in the daily soil moisture and precipitation, respectively, from dry and wet experiments with respect to the control experiments, during the runs JJAS 2003 and JJAS 2004. To compute the changes of daily soil moisture, we considered the second top soil layer in CLM4.5 (from 0 to 2.80 cm). In general, the impacts of soil moisture initial conditions on the daily soil moisture persist from three to four months over the studied domains (Fig.6). The strongest duration and amplitude of the impact on the daily soil moisture is found over the West Sahel sub-region. The impact on the daily soil moisture lasts four months in JJAS 2003 and JJAS 2004. For wet experiments, the weakest duration of the impact of soil moisture initial conditions is found over the Guinea Coast and lasts three months (Fig. 6c). While, for dry experiments, the weakest impact on the daily soil moisture is found over Central Sahel and lasted three months (Fig. 6a). These results are in line with previous works which argued that the soil moisture-atmosphere feedback strength and the land memory are place dependent (Vinnikov et al. 1996; Vinnikov and Yeserkepova 1991).

Figure 7 shows the changes of the daily precipitation to the soil moisture initial conditions over the different studied domains. The impact of the wet experiments on daily precipitation is greater in magnitude than that of dry experiments over most studied domains (Fig. 7). For dry experiments, the strongest daily precipitation response (about  $-4\text{mm.day}^{-1}$ ), is found over the Guinea Coast in the run JJAS 2003 (Fig. 7c). While for the wet experiments, the strongest impact on the daily precipitation is more than  $8\text{mm.day}^{-1}$  and it is found over the West Sahel and the Guinea Coast (Fig. 7b, c, respectively). It is worth to note that the impact of initial soil moisture conditions on daily precipitation is much shorter than the duration of the impact on daily soil moisture. The significant impact on daily precipitation is found only for wet experiments, and did not last more than 15 days in large parts of the study domain, excepted over wetter sub-



region of Guinea Coast where it lasts approximately one month. We noted that the precipitation peaks over West Sahel and Guinea Coast (Fig. 7b and c, respectively) during August and September coincide with fluctuation in the daily soil moisture impact (Fig.6b and c). This probably indicates the strong feedback of soil moisture and precipitation during this period over the Guinea Coast and West Sahel regions.

To investigate the causes of the precipitation changes, we examined the vertical profile change in relative humidity and air temperature for the runs JJAS 2003 and JJAS 2004, respectively, from dry and wet experiments with respect their control experiment.

The impacts on relative humidity and air temperature (Fig.8 and Fig.9, respectively) of soil moisture initial conditions are significant in the lower troposphere. In the low and mid-troposphere, a drying and a warming are found in the dry experiments, while a moistening and a cooling are simulated in the wet experiments. This indicates that a weak (strong) dry convection is found over most of the studied domains for dry (wet) experiments. The strongest impact on the relative humidity and temperature in the lower and middle troposphere is found over central Sahel (Fig.8a and Fig. 9a).

For the upper troposphere, the significant impact on relative humidity and temperature is found only for wet experiments, and exhibited a drying and a warming over most of studied domains (Fig.8 and Fig.9). This impact for the wet experiments was also reported by Hong and Pal (2000).

To understand other causes of the precipitation changes illustrated in Fig. 4, we analyzed the changes in lower tropospheric wind (850hpa) and specific humidity for the runs JJAS 2003 and JJAS 2004 during the dry and wet experiments with respect to the control experiments (Fig. 10).

For the dry experiments (Fig. 10a, c), we found that the moistening of the lower atmosphere decreases over most of the study domain. However, the strong wind magnitude changes over the Atlantic Ocean bring the moistening from the ocean to the Guinea Coast and West Sahel. This can explain the precipitation increase over these sub-regions in the dry experiments. Over Central Sahel, the strong decrease in precipitation seems to be associated with the decrease of specific humidity which is particularly notable in the run JJAS 2003 (Fig.4a). Conversely, for the wet experiments (Fig.10b, d), an increase in the moistening of the atmosphere is found mainly over the Sahel band while further South, a decrease of the specific humidity is simulated over Guinea Coast. The strong change in wind magnitude shifts the moistening from the North to the South, leading to precipitation increase over most part of study domain (Fig.4 b and d). These results are broadly consistent with precipitation changes for dry and wet experiments shown in Figure 4.

Summarizing these results, the impact of soil moisture initial conditions is linear only over the Central Sahel for the runs JJAS 2003 and 2004. The strongest precipitation decrease is found over Central Sahel for the dry experiment in the run JJAS 2003 with maximum change reaching -4%. While, the strongest precipitation increase is found over the West Sahel for the wet experiment in the run JJAS 2004 with maximum change about 40%. The impact of soil moisture initial conditions on daily soil moisture can persist for three to four months according to the sub-domains, while the significant impact on precipitation (greater than  $1\text{mm.day}^{-1}$ ) is much shorter and no longer than one month. The impact of soil moisture initial conditions is mostly confined at the near-surface climate and somewhat at the upper troposphere.

### 3.2. Influence on temperature and other surface fluxes.

Figure 11 shows the spatial distribution of the mean observed 2m temperature from CRU during JJAS 2003 and JJAS 2004 (Fig. 11a, c, respectively) and the mean simulated temperature from the control experiments of runs JJAS 2003 and JJAS 2004 (Fig.11 b, d, respectively) initialized with ERA20C. Table 3 summarizes the PCC and MB between model simulations of temperature with respect to CRU, calculated for the West Sahel, Central Sahel, Guinea Coast and the entire West African domain. The CRU temperature displays a zonal distribution over the whole West Africa domain. Maximum values of approximately  $34\text{ }^{\circ}\text{C}$  are found over the Sahara, while the lowest temperatures not exceed  $26^{\circ}\text{C}$ , are located over the Guinea Coast especially in orographic regions such as Guinean highlands, Cameroon Mountains and the Jos Plateau. The control experiments (Fig. 11b, d) showed good agreement in the representation of the large-scale pattern of CRU observation, with PCC about 0.99 for both JJAS 2003 and JJAS 2004 (Table 3), including the meridional gradient between Sahara Desert and Guinea Coast which is crucial for the African Easterly Jet evolution and formation (Thorncroft and Blackburn 1999; Cook 1999). The spatial extent of temperature maxima and minima are well reproduced by control experiments, however their magnitudes are overestimated compared to CRU. The strongest warm MB of control experiments relative to CRU are approximately  $2.68\text{ }^{\circ}\text{C}$  and  $2.14\text{ }^{\circ}\text{C}$  respectively for JJAS 2003 and JJAS 2004; they are found over the West Sahel (Table 3).

Figure 12 shows changes in mean temperature for the runs JJAS 2003 and JJAS 2004 of dry and wet experiments with respect to the control experiments. The dots show areas where impacts of soil moisture initial condition are statistically significant at the 0.05 level. In the dry experiments, for both JJAS 2003 and JJAS 2004 runs, the warmest changes are located under the latitude  $13^{\circ}\text{N}$ , with maximum values located over the Guinea coast. For the wet experiments, the coolest changes are found over the West and Central Sahel.

For a better quantitative evaluation, the PDF distributions of the changes in mean temperature in runs JJAS 2003 and JJAS 2004 are showed in Figure 13. The impact on temperature is linear over the Central Sahel, Guinea Coast and the whole West African domain (Fig.13a, c and d). The strongest mean temperature decrease is observed over the Central and West Sahel in wet experiences with the maximum change approximately  $-1.5^{\circ}\text{C}$  (Table 2). However, the strongest increase of mean temperature is found over the Central Sahel (JJAS 2003) and the Guinea coast (JJAS 2004) in dry experiments reaching  $0.56^{\circ}\text{C}$  and  $0.59^{\circ}\text{C}$ , respectively (Table 2). Overall, the impact in the dry (wet) sensitivity experiments on 2m-temperature showed an increase (decrease) in warming (cooling) for both JJAS 2003 and JJAS 2004 over most of the studied domains. The exception is found over the west Sahel, where both dry and wet experiments lead to temperature increase (Fig.13, Table2).

We now analyze the influence of soil moisture initial conditions anomalies on land energy balance, particularly on the surface fluxes sensible and latent heat. Figure 14 shows changes in sensible heat fluxes (in  $\text{W.m}^{-2}$ ) in runs JJAS 2003 and JJAS 2004, from dry and wet experiments compared to the control experiments. The dots show changes that are statistically significant at the 0.05 level. As shown in figure 14, the impact on sensible fluxes of soil moisture initial conditions is strong. It is linear over most of the studied domains: the dry (wet) experiments with respect to the control exhibits significant increase (decrease) of the sensible heat (Fig.14).

The PDF distributions of change in sensible heat flux are displayed in Figure 15. The dry (wet) experiments showed an increase (a decrease) of the sensible flux in both runs JJAS 2003 and JJAS 2004 (Fig. 15). The impact in wet experiments is strong over Central and West Sahel compared to the dry experiments, but not for Guinea Coast (Fig. 15, Table 2). In the dry experiments, the strongest sensible heat flux increase is found over Guinea Coast, with maximum change about  $9.18 \text{ W.m}^{-2}$  during JJAS 2004 (see Table 2). In the wet experiments, the strongest sensible heat flux decrease is located over Central Sahel with maximum change about  $-39.66 \text{ W.m}^{-2}$  during JJAS 2003 (see Table 2).

Unlike the case of sensible heat flux, changes in latent heat showed a linear opposite patterns. Dry experiments result in latent heat flux decrease, while the wet experiments result in latent heat flux increase over most of studied domains (Fig. 16). The PDF distributions of latent heat flux changes are shown in Figure 17. In the wet experiments, the strongest latent heat flux increase is found over West Sahel with maximum change reaching  $36.49 \text{ W.m}^{-2}$  in JJAS 2004 (Table2). In the dry experiments, the strongest latent heat flux decrease is located over Guinea Coast with maximum change reaching  $-14.64 \text{ W.m}^{-2}$  in JJAS 2004 (Table2). It is worth to note

that the impacts on latent and sensible heat flux in wet experiments are stronger compared to those in the dry experiments over most of studied domains, except over Guinea Coast (Table 2).

To determine whether most changes in energy go to evaporating water or to heating in the surface boundary layer, we analyzed changes in Bowen ratio in runs JJAS 2003 and JJAS 2004, for dry and wet experiments with respect to the control experiments (Fig. 18). The dots display areas with statistically significant differences at the 0.05 level. The soil moisture initial conditions strongly impact the Bowen ratio. Under the latitude 15°N, in the dry (wet) experiment, the Bowen ratio values are in the range [0,1] ([-1;0]) meaning that the dry (wet) experiments lead to an increase (decrease) of energy going to evaporate water. The exception is found only over the West Sahel (Fig.18b). In the dry (wet) experiments, the areas with increase (decrease) of energy going to evaporate water coincide with the areas of increase (decrease) of temperature. However, over the Sahara and the West Sahel, most of energy is going to heating, with Bowen ratio values out of the range [-1;1].

For a quantitative evaluation, the PDF distribution of the Bowen ratio is showed on Figure 19. In the wet experiments, the decrease of Bowen ratio is associated with a decrease in the sensible heat flux with the highest changes of energy conversion to heating simulated over West Sahel in the run JJAS 2003. In the other subdomains, latent heat flux presents a higher increase than than sensible heat flux which decreases compared to the control (Fig.19, Table 2). In the dry experiments, there is an increase of sensible heat flux in the whole domain associated with an increase of latent heat flux.

We then examined the impact on the stability of the PBL of the soil moisture initial conditions. Different spatial distributions of surface fluxes significantly affect the boundary layer development. Soil moisture can influence rainfall by limiting evapotranspiration, which affects the development of the daytime PBL and thereby the initiation and intensity of convective precipitation (Eltahir, 1998). Figure 20 shows changes in PBL (in m) for JJAS 2003 and JJAS 2004, from dry and wet experiments with respect to the control experiments with dotted areas that are statistically significant at the 0.05 level. The soil moisture initial conditions impact significantly the PBL. The dry experiments show PBL increase under the latitude 15 °N for both JJAS 2003 and JJAS 2004 (Fig.20 a and c, respectively). For the wet experiments, a PBL decrease is found over most of the studied domains. The PDF of PBL changes (Fig. 21) show that the impact on PBL is linear over most of studied domains. The dry (wet) experiments lead to an increase (decrease) of PBL for both JJAS 2003 and JJAS 2004. The strongest PBL increase

(decrease) is found over Guinea Coast (West Sahel) in dry (wet) experiments during JJAS 2004 (JJAS 2003) reaching 146.80m (−293.23m). A dry (wet) air is located above the areas where PBL increase (decrease), causing the air column to become warm (cool) and dry (moist) for the dry (wet) experiment (see Fig. 8 and Fig. 9). These results are consistent with the work of Hong and Pan (2000).

Summarizing the results of this section, we found that in the wet experiments, the cooling of the mean temperature is associated with an increase of the latent heat flux, a decrease of the sensible heat flux and of the PBL depth over most studied domain. Conversely, in the dry experiments, the warming of surface temperature is associated with a decrease of latent heat, an increase of sensible heat flux and of PBL depth.

#### 4. Conclusion

The impact of the soil moisture initial conditions on the subsequent summer (JJAS) mean climate over West Africa was explored using the RegCM4-CLM45. In particular, the aim of this study was to investigate how soil moisture initialization at the beginning of the rainy season may affect the intra-seasonal variability of temperature and precipitation mean within the subsequent season (June to September).

For this purpose, we set up three numerical experiments with RegCM4 in which we applied, at the first day (June 1<sup>st</sup>), a control soil moisture initial condition (control experiment), a wet soil moisture initial condition (wet experiment), and a dry soil moisture initial condition (dry experiment). For each experiment, an ensemble of five simulations beginning from June 1<sup>st</sup> to September 30<sup>th</sup>(JJAS), for the years 2001 to 2005 is performed. In this paper, we present results of the two runs JJAS 2003 and JJAS 2004 most impacted by soil moisture dry and wet initial conditions respectively to avoid effects of initial soil moisture internal forcing.

The impact of soil moisture initial conditions on precipitation is linear only over the Central Sahel for both JJAS 2003 and JJAS 2004, and over the West Sahel especially in JJAS 2004. In the dry experiment, the strongest precipitation decrease is found over the Central Sahel in JJAS 2003 with maximum change reaching −4% while in the wet experiment, the strongest precipitation increase is found over the West Sahel in JJAS 2004 with maximum change reaching 40%. The impact of soil moisture initial conditions can persist for three to four months (90-120 days) depending on the sub-region but the impact on precipitation is no longer than 30 days (15 days over the Sahel and 30 days over the Guinea Sahel).

Our results show that soil moisture wet initial conditions lead in the lower troposphere to an increase of relative humidity associated with a cooling of air temperature and in the upper troposphere, to a decrease of relative humidity and a warming of air temperature. While the dry experiments mainly impact the lower troposphere with a decrease of the relative humidity associated with a warming air temperature.

The temperature at 2m is more sensitive to the anomalies of initial soil moisture condition than the precipitation. The strongest impact on 2m-temperature is found over the Central Sahel with a maximum change about  $-1.5^{\circ}\text{C}$  and  $0.6^{\circ}\text{C}$  for the wet and dry experiments, respectively.

Our study showed significant impacts of soil moisture initial conditions on the surface energy fluxes. For the wet experiments, we found that the cooling of surface temperature is associated with a decrease of the sensible heat flux, an increase of the latent heat flux and a decrease of the PBL depth. For the dry experiments, the warming of surface temperature is associated with a increase of the sensible heat flux, a decrease of the latent heat flux and an increase of the PBL depth.

This study showed that soil moisture as a boundary condition plays a major role in controlling summer climate variability not only over the Sahel band but also over humid zones such as Guinea Coast. Therefore, the good prescription of soil moisture initial conditions could improve the simulation of precipitation and temperature, which would help to reduce biases in climate model simulations. Overall, land surface initialization can contribute to improving sub-seasonal to seasonal forecast skill, but this requires further investigation. We recognize that

This study is the first investigating the impact of soil moisture initial conditions in West Africa. However, this study is based on idealized experiments : sensitivity experiments such as "wet" and "dry" ones conducted in this study were not intended to simulate real climate since such extremes are very rare. Moreover, this study is very specific to RegCM4. In the future, an investigation using different RCMs in a multi-model framework will contribute to better quantify the impact of soil moisture initial conditions. At shorter timescales, there is a need to understand how the soil moisture initial conditions contribute to the triggering and the maintenance of the mesoscale convective systems which are known to explain large amount of rainfall in the region (Mathon et al., 2002). Finally, in the context of climate change, considering the projected increase of high-impact weather events in the region, there is a need to explore the sensitivity of soil moisture initial conditions to climate extremes.



#### **Authors contributions**

The authors declare to have no conflict of interest with this work. B. Koné and A. Diedhiou fixed the analysis framework. B. Koné carried out all the simulations and figures production according to the outline proposed by A. Diedhiou. B. Koné and A. Diedhiou, S. Anquetin and A. Diawara worked on the analyses. All authors contributed to the drafting of this manuscript.

#### **Acknowledgements**

The research leading to this publication is co-funded by the NERC/DFID “Future Climate for Africa” programme under the AMMA-2050 project, grant number NE/M019969/1 and by IRD (Institut de Recherche pour le Développement; France) grant number UMR IGE Imputation 252RA5.

**References:**

Beljaars A. C. M., Viterbo P., Miller M. J., and Betts A. K.: The anomalous rainfall over the United States during July 1993: Sensitivity to land surface parameterization and soil moisture anomalies, *Mon. Weather Rev.*, 124(3), 362–382, doi:10.1175/1520-0493(1996)124<0362:TAROTU>2.0.CO;2, 1996.

Bosilovich, M. G., and Sun W. Y.: Numerical simulations of the 1993 Midwestern flood: Land–atmosphere interactions. *J. Climate*, 12, 1490–1505, 1999.

Cook K. H.: Generation of the African easterly jet and its role in determining West African precipitation, *J. Climate*, 12, 1165–1184, [https://doi.org/10.1175/1520-0442\(1999\)012<1165:GOTAEJ>2.0.CO;2](https://doi.org/10.1175/1520-0442(1999)012<1165:GOTAEJ>2.0.CO;2), 1999.

Damien Decremet, Chul E. Chung, Annica M. L. Ekman & Jenny Brandefelt (2014) Which significance test performs the best in climate simulations?, *Tellus A: Dynamic Meteorology and Oceanography*, 66:1, DOI: 10.3402/tellusa.v66.23139.

Danielson J.J., and Gesch D.B.: Global multi-resolution terrain elevation data 2010 (GMTED2010): U.S. Geological Survey Open-File Report 2011–1073, 26 p, 2011.

Dirmeyer P. A., Koster R. D., and Guo Z.: Do global models properly represent the feedback between land and atmosphere, *J. Hydrometeorol.*, 7(6), 1177–1198, doi:10.1175/JHM532.1, 2006.

Douville, F. Chauvin, and H. Broqua.: Influence of soil moisture on the Asian and African monsoons. Part I: Mean monsoon and daily precipitation. *J. Climate*, 14, 2381–2403, 2001.

Eltahir E. A. B.: A soil moisture-rainfall feedback mechanism 1. Theory and observations, *Water Resour. Res.*, 34, 765–776, doi:10.1029/97WR03499, 1998.

Emanuel K. A.: A scheme for representing cumulus convection in large-scale models. *Journal of the Atmospheric Science* 48: 2313–2335, 1991.

Funk, C., Peterson, P., Landsfeld, M. et al. The climate hazards infrared precipitation with stations—a new environmental record for monitoring extremes. *Sci Data* 2, 150066 (2015). <https://doi.org/10.1038/sdata.2015.66>

Gao, X.-J., Shi, Y., and Giorgi, F.: Comparison of convective parameterizations in RegCM4 experiments over China with CLM as the land surface model, *Atmos. Ocean. Sci. Lett.*, 9, 246–254, <https://doi.org/10.1080/16742834.2016.1172938>, 2016.

Giorgi F., Coppola E., Solmon F., Mariotti L., Sylla M. B., Bi X., Elguindi N., Diro G. T., Nair V., Giuliani G., Cozzini S., Guettler I., O’Brien T., Tawfik A., Shalaby A., Zakey A. S., Steiner A., Stordal F., Sloan L., and Brankovic C.: RegCM4: model description and preliminary tests over multiple CORDEX domains, *Clim. Res.*, 52, 7–29, <https://doi.org/10.3354/cr01018>, 2012.

Grell G., Dudhia J. and Stauffer D. R.: A description of the fifth generation Penn State/NCAR Mesoscale Model (MM5), National Center for Atmospheric Research Tech Note NCAR/TN-398+STR, NCAR, Boulder, CO, 1994.

Harris I., Jones P. D., Osborn T. J. and Lister D. H.: Updated high-resolution grids of monthly climatic observations, *Int. J. Climatol.*, 34, 623–642, <https://doi.org/10.1002/joc.3711>, 2013.

Holtzlag A., De Bruijn E., and Pan H. L.: A high resolution air mass transformation model for short-range weather forecasting, *Mon. Weather Rev.*, 118, 1561–1575, 1990.

Hong S-Y. and Pan H-L.: Impact of soil moisture anomalies on seasonal, summertime circulation over North America in a regional climate model. *J. Geophys. Res.*, 105 (D24), 29 625–29 634, 2000.

555 Jaeger E. B., and Seneviratne S.I.: Impact of soil moisture-atmosphere coupling on European  
556 climate extremes and trends in a regional climate model, *Clim. Dyn.*, 36(9-10), 1919-1939,  
557 doi:10.1007/s00382-010-0780-8, 2011.

558

559 Kang S, Im E.-S. and Ahn J.-B.: The impact of two land-surface schemes on the characteristics  
560 of summer precipitation over East Asia from the RegCM4 simulations *Int. J. Climatol.* 34: 3986-  
561 3997, 2014.

562

563 Kiehl J., Hack J., Bonan G., Boville B., Breigleb B., Williamson D., Rasch P.; Description of the  
564 NCAR Community Climate Model (CCM3). National Center for Atmospheric Research Tech  
565 Note NCAR/TN-420+STR, NCAR, Boulder, CO, 1996.

566

567 Kim J-E., and Hong S-Y.: Impact of Soil Moisture Anomalies on Summer Rainfall over East  
568 Asia: A Regional Climate Model Study, *Journal of Climate*. Vol. 20, 5732–5743, DOI:  
569 10.1175/2006JCLI1358.1, 2006.

570

571 Kirtman B.P., Schopf P. S.: Decadal Variability in ENSO Predictability and Prediction. *Journal*  
572 *of Clim.* 11, 2804, 1998.

573

574 Koné B., Diedhiou A., N’datchoh E. T., Sylla M. B., Giorgi F., Anquetin S., Bamba A., Diawara  
575 A., and Kobea A. T.: Sensitivity study of the regional climate model RegCM4 to different  
576 convective schemes over West Africa. *Earth Syst. Dynam.*, 9, 1261–1278.  
577 <https://doi.org/10.5194/esd-9-1261-2018>, 2018.

578

579 Koster R. D., Dirmeyer P. A., Zhichang G., Bonan G., Chan E., Cox P., Gordon C. T., Kanae S.,  
580 Kowalczyk E., Lawrence D., Liu P., Lu C. H, Malyshev S., McAvaney B., Mitchell K, Mocko  
581 D., Oki T., Oleson K., Pitman A., Sud Y. C., Taylor C. M., Versegghy D., Vasic R., Xue Y.,  
582 Yamada T.: Regions of strong coupling between soil moisture and precipitation, *Science*, 305,  
583 1138–1140, doi:10.1126/science.1100217, 2004.

584

585 Lawrence D.M., Oleson K.W., Flanner M.G., Thornton P.E., Swenson S.C., Lawrence P.J., Zeng  
586 X., Yang Z.-L., Levis S., Sakaguchi K., Bonan G.B., and Slater A.G.:Parameterization  
587 improvements and functional and structuraladvances in version 4 of the Community Land  
588 Model. *J. Adv. Model. Earth Sys.* 3. DOI:10.1029/2011MS000045, 2011.

- Liu D., Wang G. L., Mei R., Yu Z. B. and Gu H. H.: Diagnosing the strength of land-atmosphere coupling at sub-seasonal to seasonal time scales in Asia, *J. Hydrometeor.*, doi:10.1175/JHM-D-13-0104.1, 2013.
- Liu D., G. Wang R. Mei Z. Yu, and Yu M.: Impact of soil moisture initial conditions anomalies on climate mean and extremes over Asia, *J. Geophys. Res. Atmos.*, 119, 529–545, doi:10.1002/2013JD020890, 2014.
- Loveland, T. R., Reed, B. C., Brown, J. F., Ohlen, D. O., Zhu, J., Yang, L., and Merchant, J. W.: Development of a global land cover characteristics database and IGBP DISCover from 1-km AVHRR Data, *Int. J. Remote. Sens.*, 21, 1303–1330, 2000.
- Mathon, V., Diedhiou, A., & Laurent, H. (2002). Relationship between easterly waves and mesoscale convective systems over the Sahel. *Geophysical research letters*, 29(8), 57-1.
- Menéndez, C. G., Giles, J., Ruscica, R., Zaninelli, P., Coronato, T., Falco, M., ... & Li, L. (2019). Temperature variability and soil–atmosphere interaction in South America simulated by two regional climate models. *Climate Dynamics*, 53(5), 2919-2930.
- Oglesby R. J., and Erickson III D. J.: Soil moisture and the persistence of North American drought. *J. Climate*, 2, 1362–1380, 1989.
- Oglesby R. J., Marshall S., Erickson III D. J., Roads J. O. and Robertson F. R.: Thresholds in atmosphere-soil moisture interactions: Results from climate model studies. *J. Geophys. Res.*, 107, 4244, doi:10.1029/2001JD001045, 2002.
- Oleson K., Lawrence D. M., Bonan G. B., Drewniak B., Huang M., Koven C. D., Yang Z. -L.: Technical description of version 4.5 of the Community Land Model (CLM) (No. NCAR/TN-503+STR). doi:10.5065/D6RR1W7M, 2013.
- Paeth H., Girmes R., Menz G. and Hense A.: Improving seasonal forecasting in the low latitudes, *Mon. Weather Rev.*, 134, 1859-1879, 2006.

Pal J. S., Small E. E. and Elthair E. A.: Simulation of regional scale water and energy budgets: representation of subgrid cloud and precipitation processes within RegCM, *J. Geophys. Res.*, 105, 29579–29594, 2000.

Pal J. S. and Eltahir E. A. B.: Pathways relating soil moisture conditions to future summer rainfall within a model of the land–atmosphere system. *J. Climate*, 14, 1227–1242, 2001.

Peterson T. C., Folland C., Gruza G., Hogg W. Mokssit A., Plummer N.: Report on the activities of the working group on climate change detection and related rapporteurs 1998-2001. Geneva (Switzerland): WMO Rep. WCDMP 47, WMO-TD 1071, 2001.

Nicholson S. E.: The West African Sahel: a review of recent studies on the rainfall regime and its interannual variability, *Meteorology*, 453521, 32 p., <https://doi.org/10.1155/2013/453521>, 2013.

Nikulin G., Jones C., Samuelsson P., Giorgi F., Asrar G., Büchner M., Cerezo-Mota R., Christensen O. B., Déque M., Fernandez J., Hansler A., van Meijgaard E., Sylla M. B. and Sushama L.: Precipitation climatology in an ensemble of CORDEX-Africa regional climate simulations, *J. Climate*, 6057–6078, <https://doi.org/10.1175/JCLI-D-11-00375.1>, 2012.

Rasmusson E. M. and Carpenter T. H.: Variations in Tropical Sea Surface Temperature and Surface Wind Fields Associated with the Southern Oscillation/El Niño. *Mon. Weather Rev.* 110, 354, 1982.

Reynolds, R. W. and Smith, T. M.: Improved global sea surface temperature analysis using optimum interpolation, *J. Climate*, 7, 929–948, 1994.

Seager R., and Vecchi G. A.: Greenhouse warming and the 21<sup>st</sup> century hydroclimate of southwestern North America. *Proc. Natl. Acad. Sci. USA*, 107, 21 277–21 282, doi:10.1073/pnas.0910856107, 2010.

Simmons A. S., Uppala D. D. and Kobayashi S.: ERA-interim: new ECMWF reanalysis products from 1989 onwards, *ECMWF Newsl.*, 110, 29–35, 2007.



Solmon F., Giorgi F., and Lioussse C.: Aerosol modeling for regional climate studies: application to anthropogenic particles and evaluation over a European/African domain, *Tellus B*, 58, 51–72, 2006.

Sundqvist H. E., Berge E., and Kristjansson J. E.: The effects of domain choice on summer precipitation simulation and sensitivity in a regional climate model, *J. Climate*, 11, 2698-2712, 1999.

Takahashi, H. G., & Polcher, J. (2019). Weakening of rainfall intensity on wet soils over the wet Asian monsoon region using a high-resolution regional climate model. *Progress in Earth and Planetary Science*, 6(1), 1-18.

Thorncroft, C. D. and Blackburn, M.: Maintenance of the African easterly jet, *Q. J. R. Meteorol Soc.*, 125, 763–786, 1999.

Uppala S., Dee D., Kobayashi S., Berrisford P. and Simmons A.: Towards a climate data assimilation system: status update of ERA-interim, *ECMWF Newsl.*, 15, 12–18, 2008.

Vinnikov K. Y. and Yeserkepova I. B.: Soil moisture: Empirical data and model results, *J. Clim.*, 4(1), 66–79, doi:10.1175/1520-0442(1991) 004<0066:SMEDAM>2.0.CO;2, 1991.

Vinnikov K. Y., Robock A., Speranskaya N. A. and Schlosser A.: Scales of temporal and spatial variability of midlatitude soil moisture, *J. Geophys. Res.*, 101(D3), 7163–7174, doi:10.1029/95JD02753, 1996.

Wang, G., Yu, M., Pal, J. S., Mei, R., Bonan, G. B., Levis, S., and Thornton, P. E.: On the development of a coupled regional climate vegetation model RCM-CLM-CN-DV and its validation its tropical Africa, *Clim. Dynam*, 46, 515–539, 2016.

Xue Y., De Sales F., Lau K. M. W., Bonne A., Feng J., Dirmeyer P., Guo Z., Kim K. M., Kitoh A., Kumar V., Poccarr-Leclercq I., Mahowald N., Moufouma-Okia W., Pegion P., Rowell D. P., Schemm J., Schulbert S., Sealy A., Thiaw W. M., Vintzileos A., Williams S. F. and Wu M. L.: Intercomparison of West African Monsoon and its variability in the West African Monsoon

Modelling Evaluation Project (WAMME) first model Intercomparison experiment, *Clim. Dynam.*, 35, 3–27, <https://doi.org/10.1007/s00382-010-0778-2>, 2010.

Zakey A. S., Solmon F., and Giorgi F.: Implementation and testing of a desert dust module in a regional climate model, *Atmos. Chem. Phys.*, 6, 4687–4704, <https://doi.org/10.5194/acp-6-4687-2006>, 2006.

Zeng X., Zhao M. and Dickinson R. E.: Intercomparison of bulk aerodynamic algorithms for the computation of sea surface fluxes using TOGA COARE and TAO DATA, *J. Climate*, 11, 2628–2644, 1998.

Zhang, J., W.-C. Wang, and J. Wei, Assessing land-atmosphere coupling using soil moisture from the Global Land Data Assimilation System and observational precipitation, *J. Geophys. Res.*, 113, D17119, doi:10.1029/2008JD009807, 2008.

Zhang, J., W.-C. Wang, and L. R. Leung.: Contribution of land-atmosphere coupling to summer climate variability over the contiguous United States, *J. Geophys. Res.*, 113, D22109, doi:10.1029/2008JD010136, 2008.

Zhang, J. Y., L. Y. Wu, and W. Dong.: Land-atmosphere coupling and summer climate variability over East Asia, *J. Geophys. Res.*, 116, D05117, doi 10.1029/2010JD014714, 2011.

#### Tables and figures:

	Central Sahel		West Sahel		Guinea		West Africa	
	PCC	MB (%)	PCC	MB (%)	PCC	MB (%)	PCC	MB (%)
CTRL_2003	0.98	−47.97	0.87	−75.76	0.82	−47.12	<b>0.73</b>	<b>−49.31</b>
CTRL_2004	0.98	−47.89	0.87	−68.35	0.85	−51.97	<b>0.77</b>	<b>−50.56</b>

**Table1:** The pattern correlation coefficient (PCC) and the mean bias (MB) for JJAS precipitation for model simulations with respect to CHIRPS, calculated for Guinea coast, central Sahel, west Sahel and the entire West African domain during the period 2003 and 2004.

		Central Sahel		West Sahel		Guinea coast		West Africa	
		$\Delta WC$	$\Delta DC$	$\Delta WC$	$\Delta DC$	$\Delta WC$	$\Delta DC$	$\Delta WC$	$\Delta DC$
Precipitation (%)	2003	13.80	<b>-4.09</b>	29.95	6.58	19.40	9.20	8.88	4.68
	2004	15.86	-3.29	<b>38.58</b>	-1.25	26.6	12.68	10.72	7.64
Temperature mean (°C)	2003	-1.48	<b>0.56</b>	<b>-1.55</b>	-0.41	-0.15	0.54	-0.62	0.50
	2004	<b>-1.51</b>	0.47	-1.15	-0.24	-0.19	<b>0.59</b>	-0.41	0.59
Sensible heat (w.m <sup>-2</sup> )	2003	-16.89	8.57	<b>-39.66</b>	5.31	-2.41	7.52	-14.32	8.06
	2004	-19.53	7.55	-31.97	7.23	-3.01	<b>9.18</b>	-14.46	6.81
Latent heat (w.m <sup>-2</sup> )	2003	21.27	-6.67	34.21	-6.06	3.09	-13.38	15.86	-8.07
	2004	28.55	-4.81	<b>36.49</b>	-6.20	7.09	<b>-14.64</b>	19.68	-8.53
Bowen ratio	2003	-0.42	0.31	<b>-3.01</b>	-0.05	-0.03	0.12	-0.48	0.28
	2004	<b>-0.64</b>	<b>0.39</b>	-2.49	<b>0.41</b>	<b>-0.64</b>	0.15	-0.57	0.26
PBL (m)	2003	-233.49	81.23	<b>-293.23</b>	-0.16	-94.42	132.74	-128.90	75.57
	2004	-223.06	49.48	-247.08	19.87	-119.38	<b>146.80</b>	-117.69	56.53

735

736 **Table2:** Table summarizing the maximum values of change obtained from the PDF distribution

737 for precipitation, temperature, sensible heat, latent heat, Bowen ratio and PBL, calculated for

738 Guinea coast, central Sahel, west Sahel and the entire West African domain during the period

739 JJAS 2003 and JJAS 2004.

740

741

	Central Sahel		West Sahel		Guinea		West Africa	
	PCC	MB (°C)	PCC	MB (°C)	PCC	MB (°C)	PCC	MB (°C)
CTRL_2003	0.99	1.52	0.99	2.68	0.99	−0.34	0.99	0.85
CTRL_2004	0.99	1.50	0.99	2.14	0.99	−0.57	0.99	0.51

742

743 **Table3:** The pattern correlation coefficient (PCC) and the mean bias (MB) for JJAS 2m-  
744 temperature for model simulations with respect to CRU, calculated for Guinea coast, central  
745 Sahel, west Sahel and the entire West African domain during the period JJAS 2003 and JJAS  
746 2004.

747

748

749

750

751

752

753

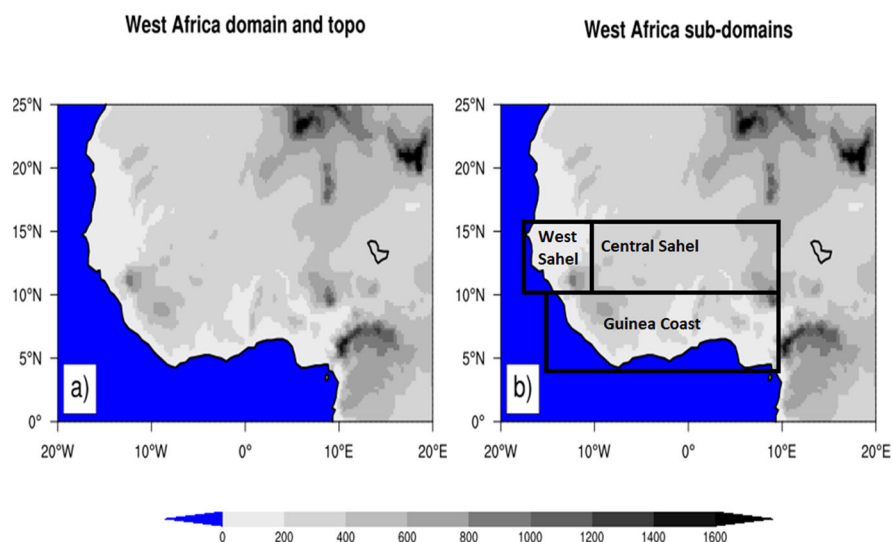


**Figure 1:** Topography of the West African domain. The analysis of the model result has an emphasis on the whole West African domain and the three sub-regions Guinea coast, central Sahel and west Sahel, which are marked with black boxes.



## West Africa

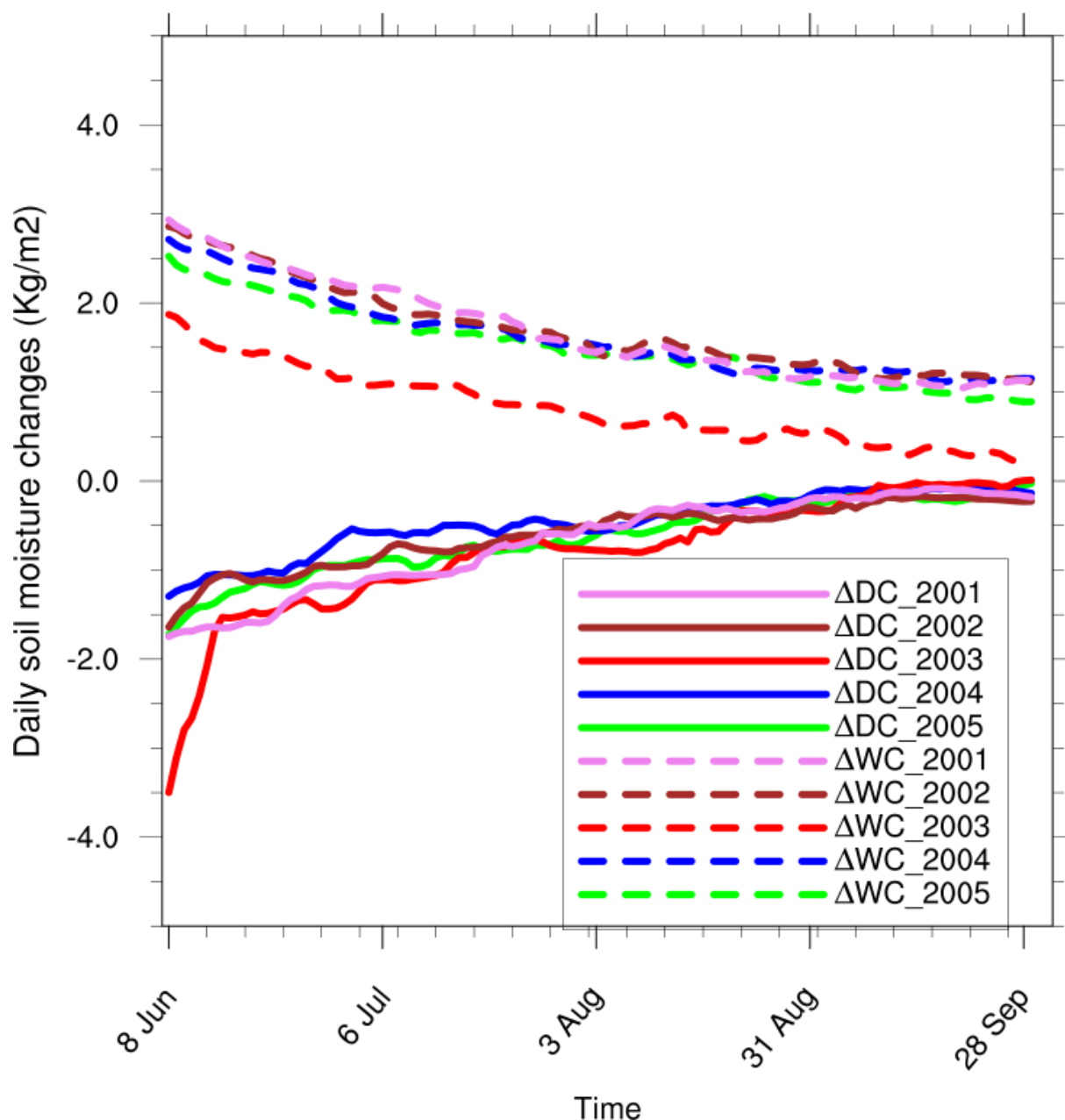


**Figure 2:** Changes in daily soil moisture in the 5 runs (JJAS 2001 to 2005) over West African domain, for the dry ( $\Delta DC$ ) and wet ( $\Delta WC$ ) experiments with respect to their corresponding control experiment.

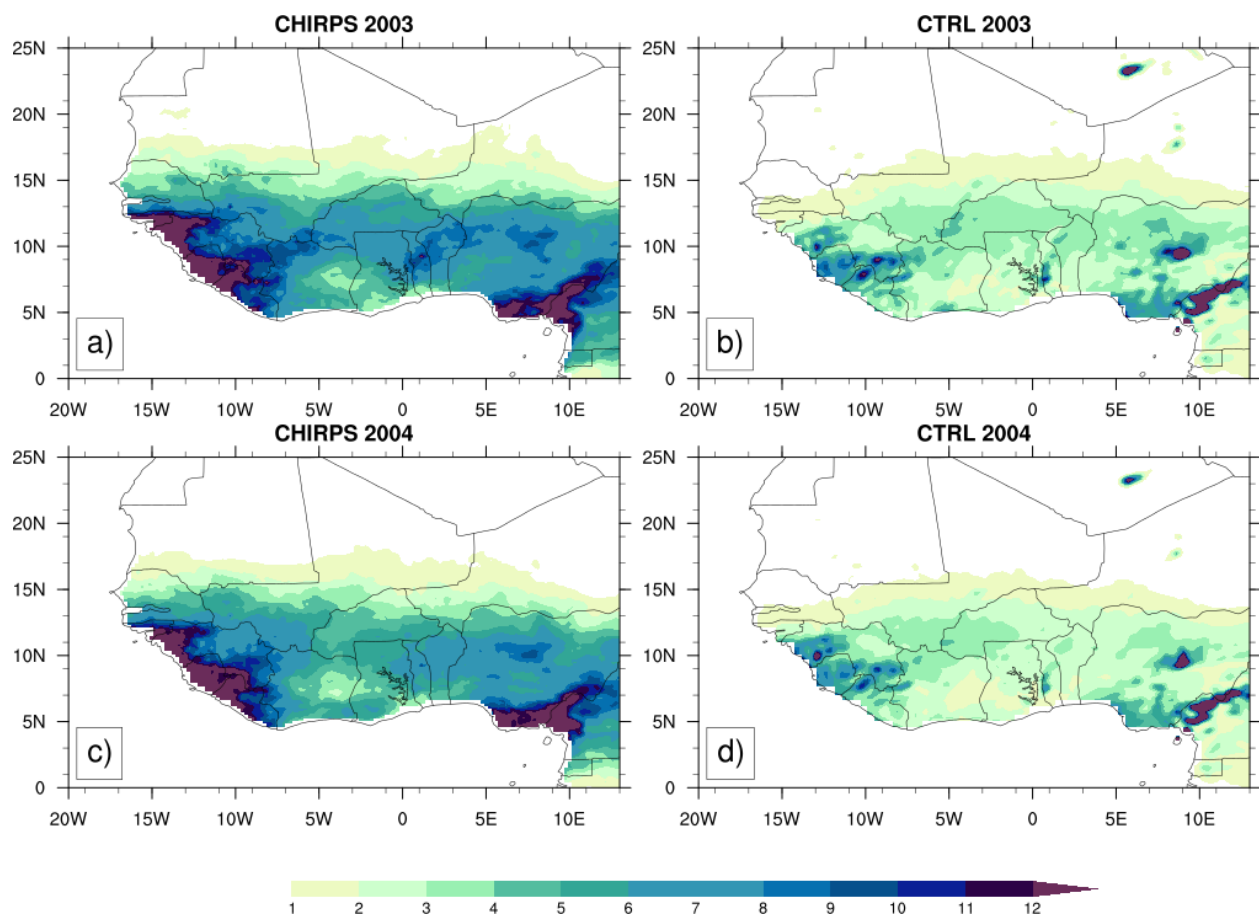


**Figure3:** Mean precipitation (mm/day) from CHIRPS (a, c) and the simulated control experiments (CTRL) (b, d) with the reanalysis initial soil moisture ERA20C during JJAS 2003 and JJAS 2004.

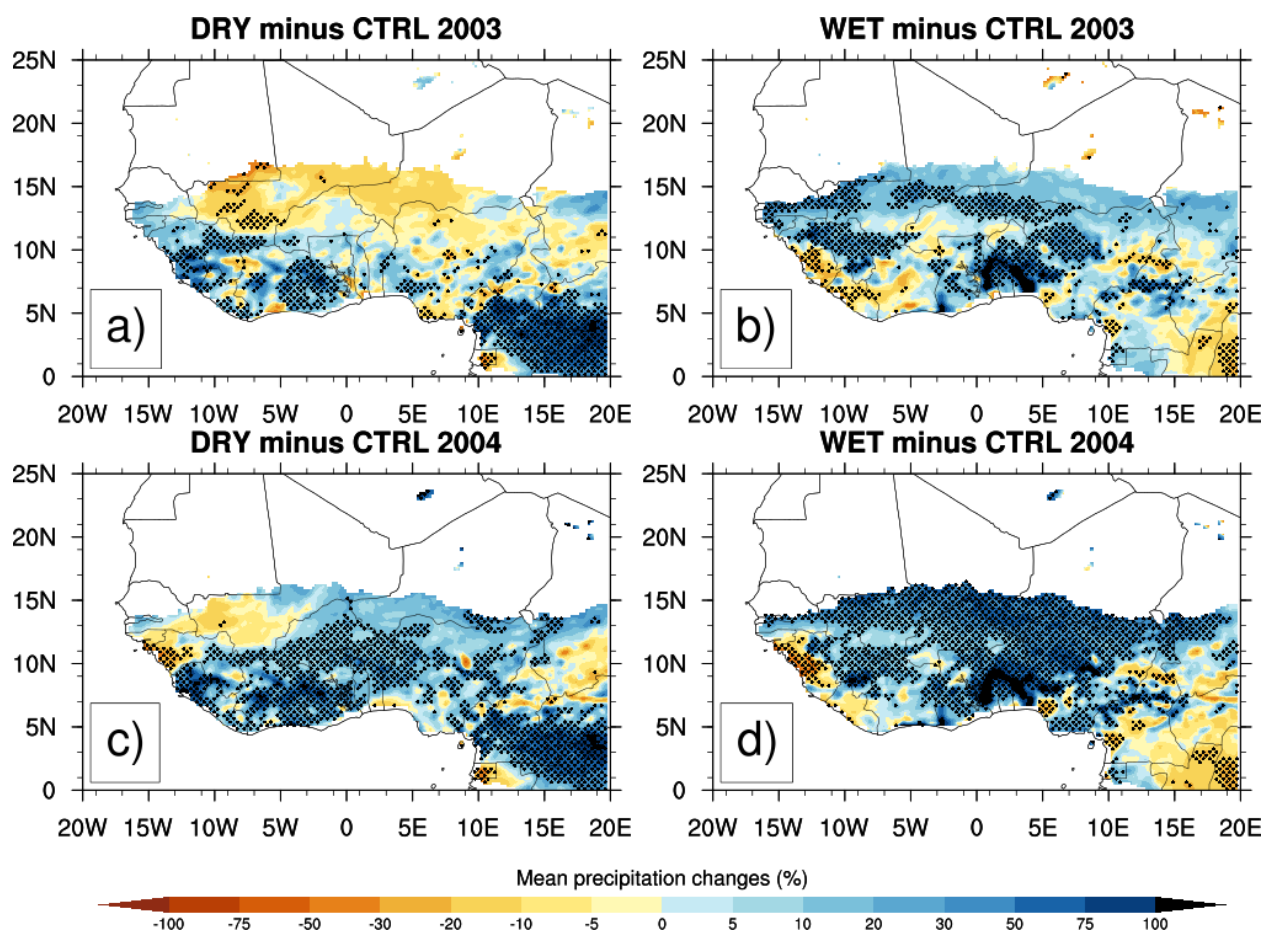


**Figure4:** Changes in mean precipitation (in %) for JJAS 2003 and JJAS 2004, from dry (resp. a and c) and wet (resp. b and d) experiments with respect to the control experiment, the dotted area shows differences that are statistically significant at 0.05 level.

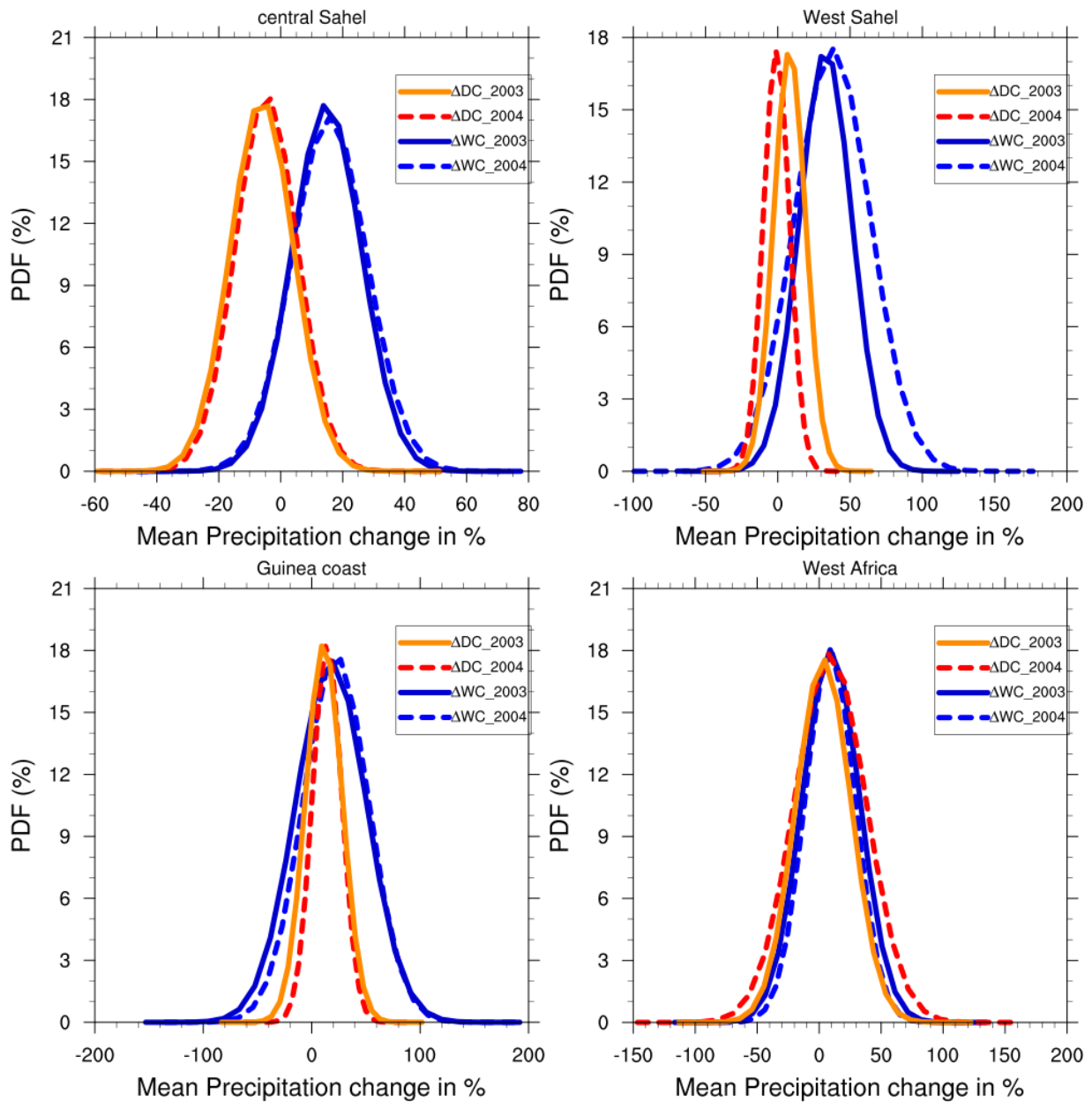
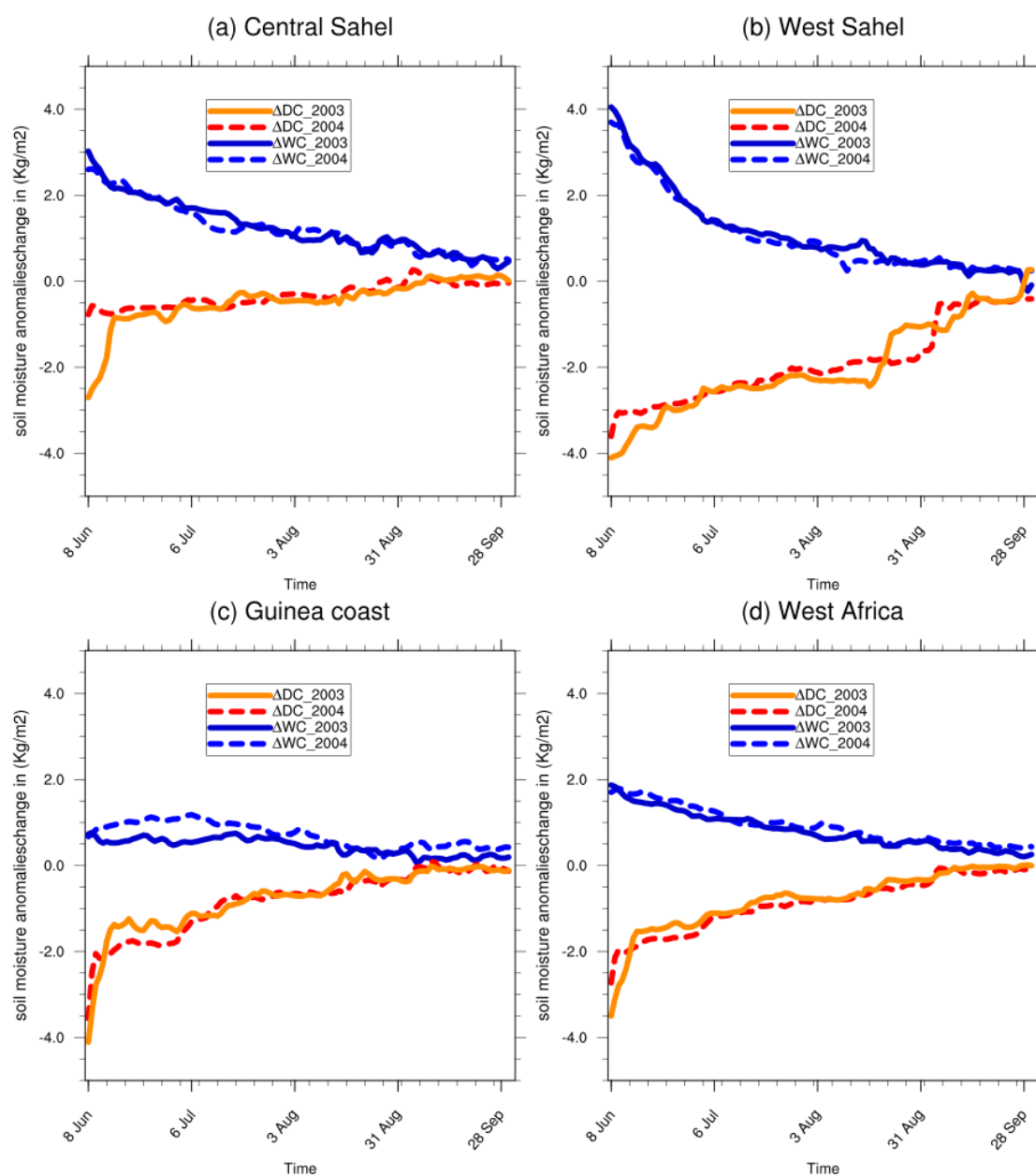


**Figure 5:** PDF distributions (%) of mean precipitation changes in JJAS 2003 and JJAS 2004, over (a) central Sahel, (b) West Sahel, (c) Guinea and (d) West Africa derived from dry ( $\Delta DC$ ) and wet ( $\Delta WC$ ) experiments compared to the control experiment.



838

839 **Figure 6:** Daily domain-average soil moisture changes for JJAS 2003 and JJAS 2004, from dry  
 840 ( $\Delta DC$ ) and wet ( $\Delta WC$ ) experiments with respect to the control experiment.

841

842

843

844

845

846

847

848

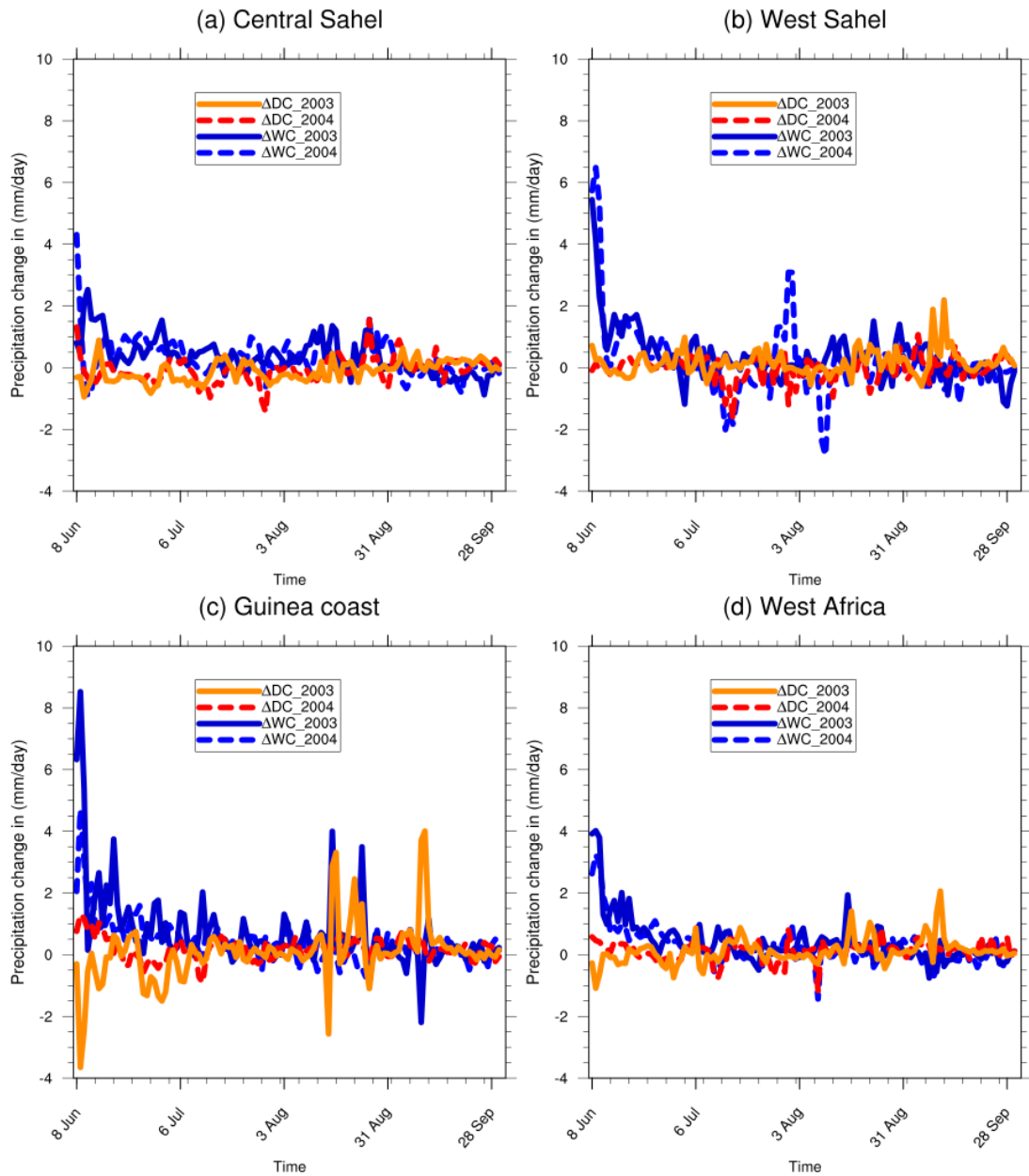


**Figure 7:** Daily domain-average precipitation changes for JJAS 2003 and JJAS 2004, from dry ( $\Delta DC$ ) and wet ( $\Delta WC$ ) experiments with respect to the control experiment.



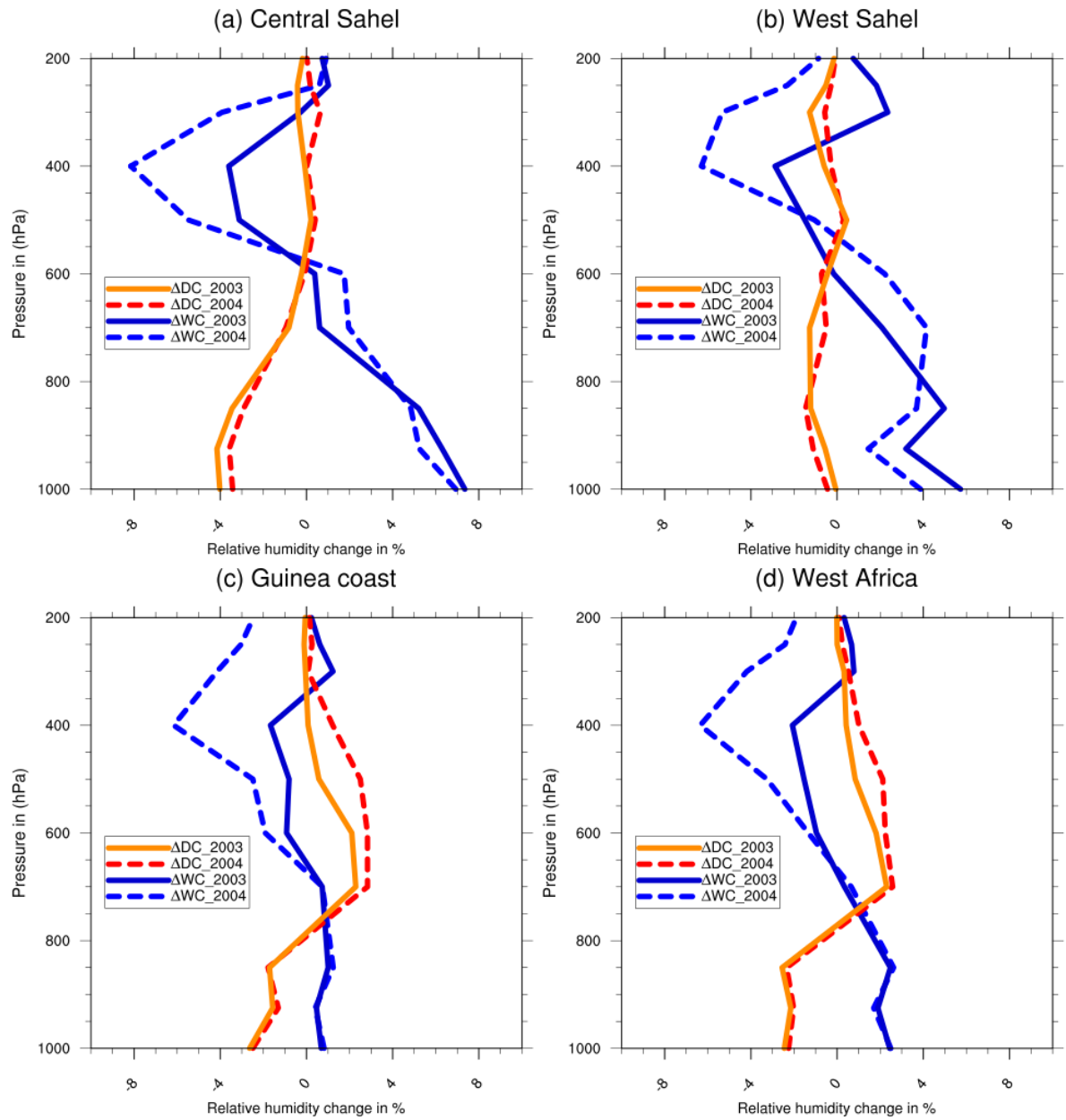


**Figure 8:** Vertical profile changes in Relative humidity for JJAS 2003 and JJAS 2004 from the dry ( $\Delta DC$ ) and wet ( $\Delta WC$ ) experiments with respect to corresponding control experiment over (a) central Sahel, (b) west Sahel, (c) Guinea coast, and (d) West Africa.

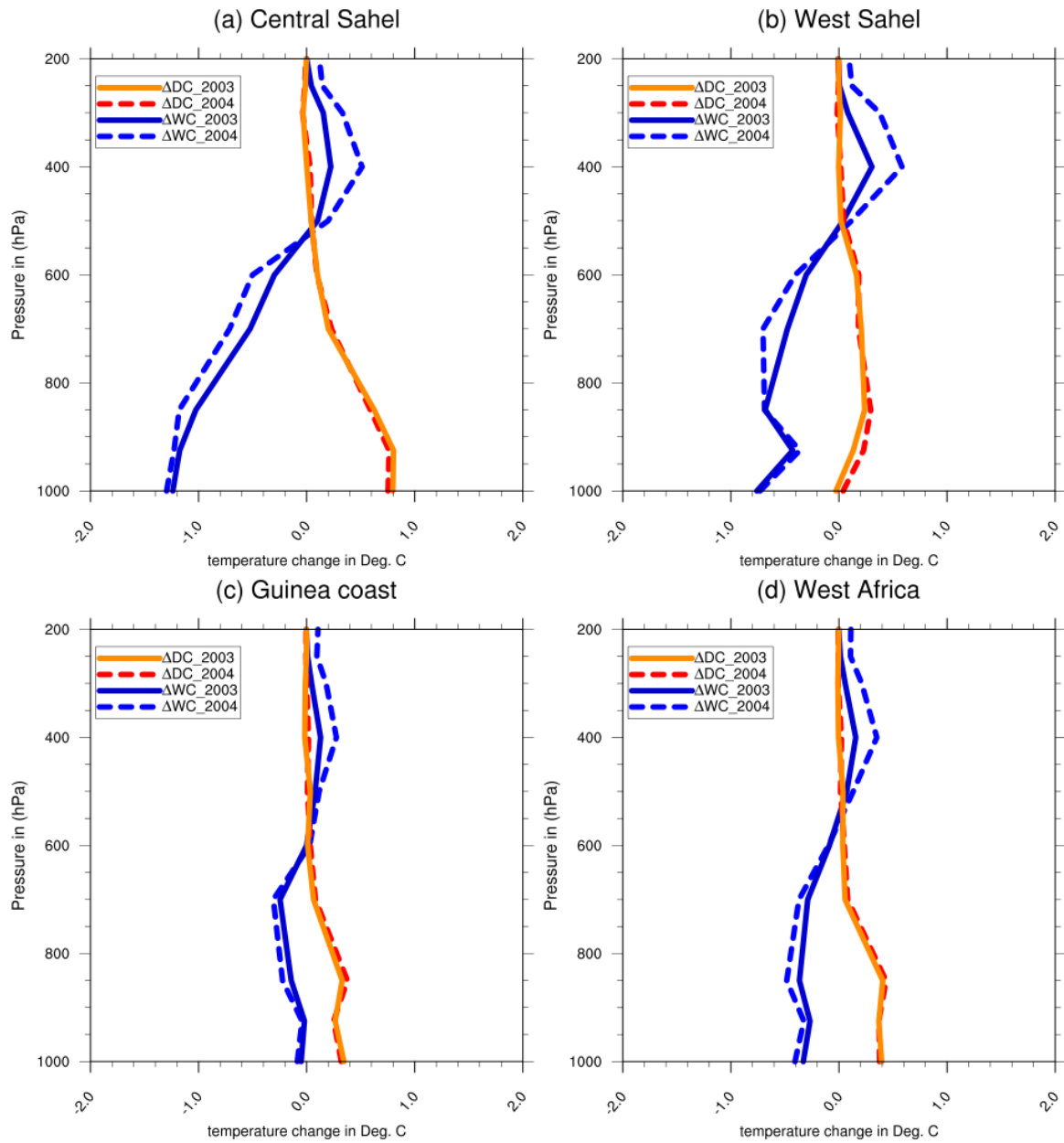


**Figure 9:** Vertical profile changes in temperature for JJAS 2003 and JJAS 2004 from the dry ( $\Delta DC$ ) and wet ( $\Delta WC$ ) experiments with respect to the control experiment over (a) central Sahel, (b) west Sahel, (c) Guinea coast, and (d) West Africa.

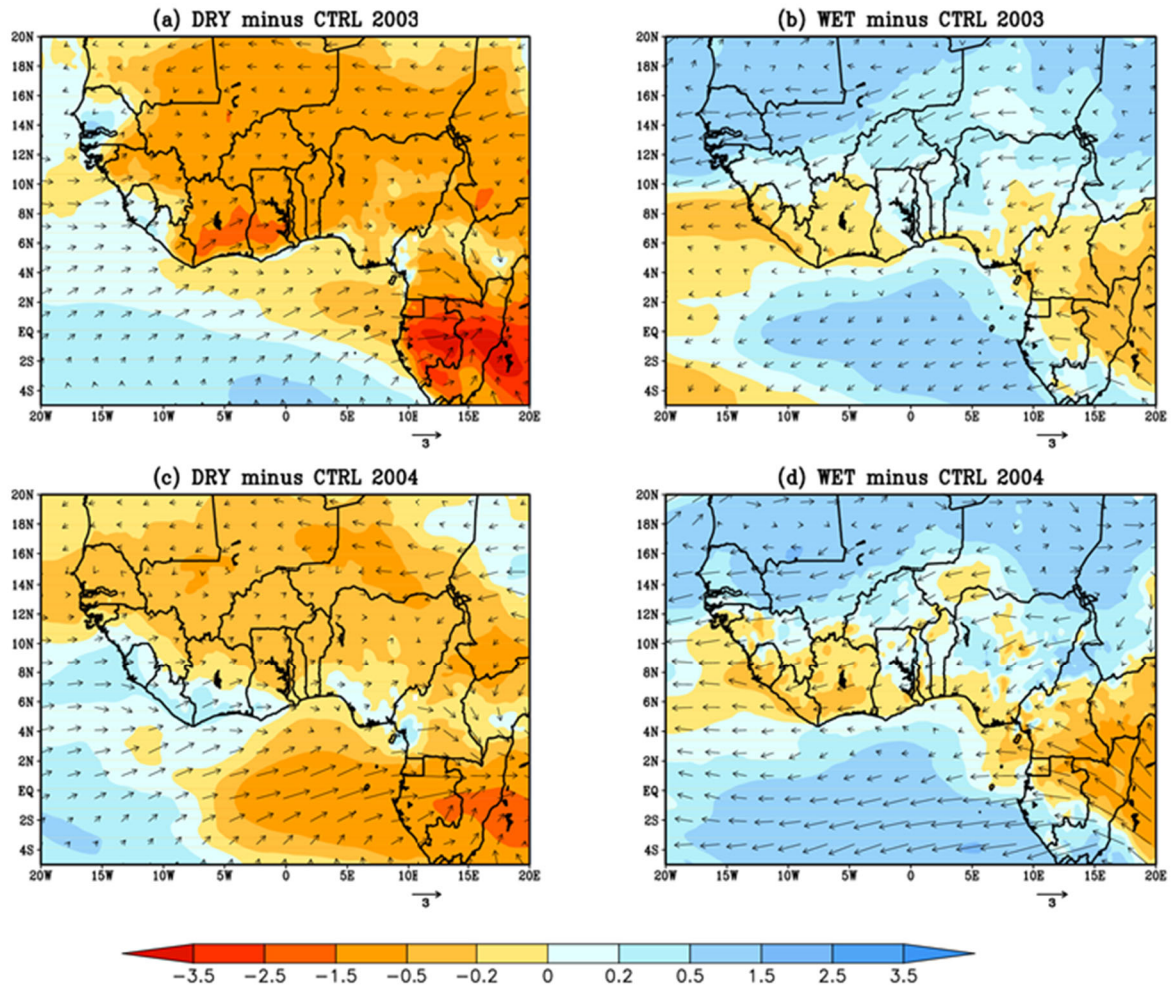


**Figure 10:** The lower tropospheric wind (850hpa) and moisture bias for JJAS 2003 and JJAS 2004 from the dry (a and c) and wet (b and d) experiments with respect to the control experiment.

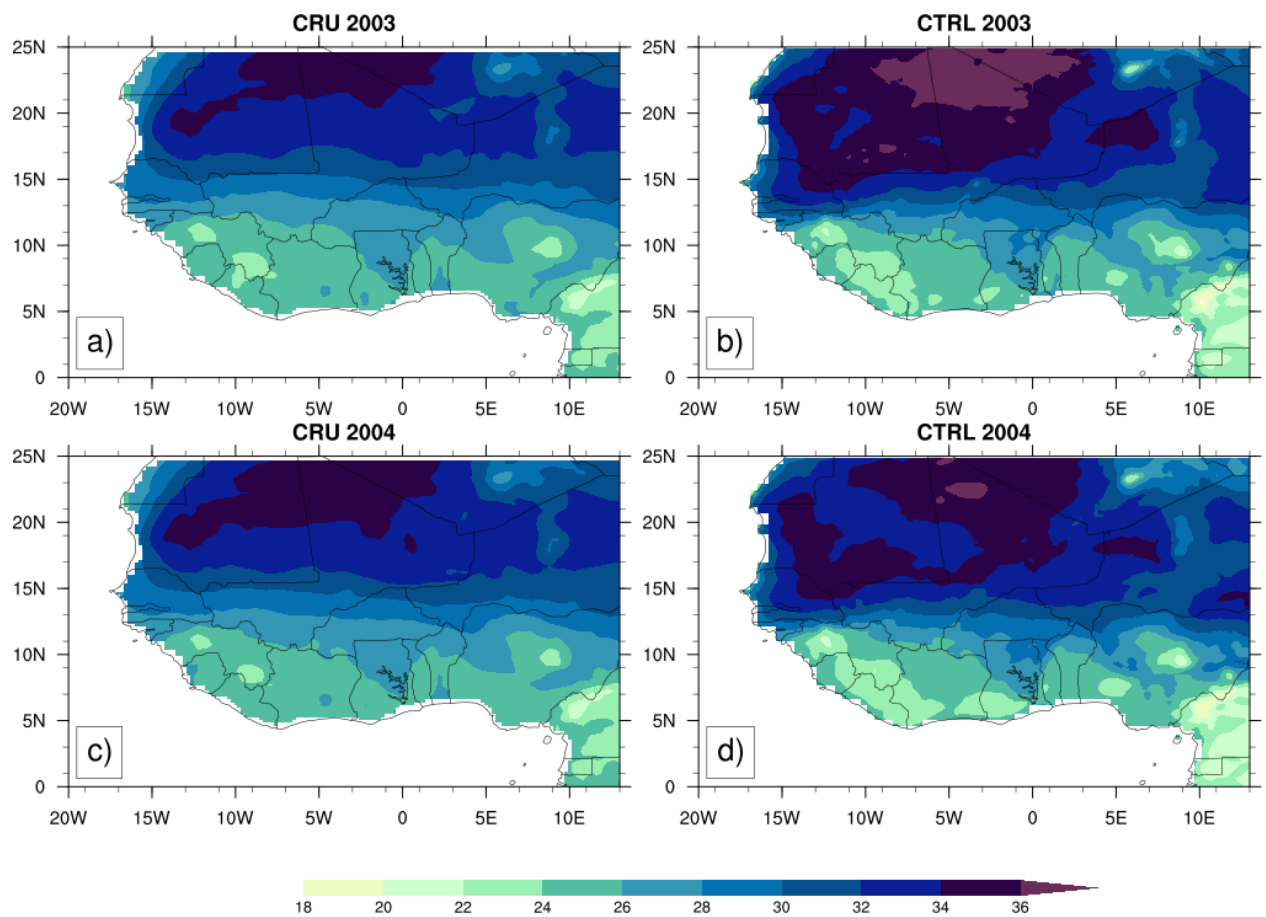


**Figure 11:** Mean 2m-temperature (°C) from CRU (a and c) for JJAS 2003 and JJAS 2004 and the simulated control experiment (b and d) with the reanalysis initial soil moisture ERA20C.

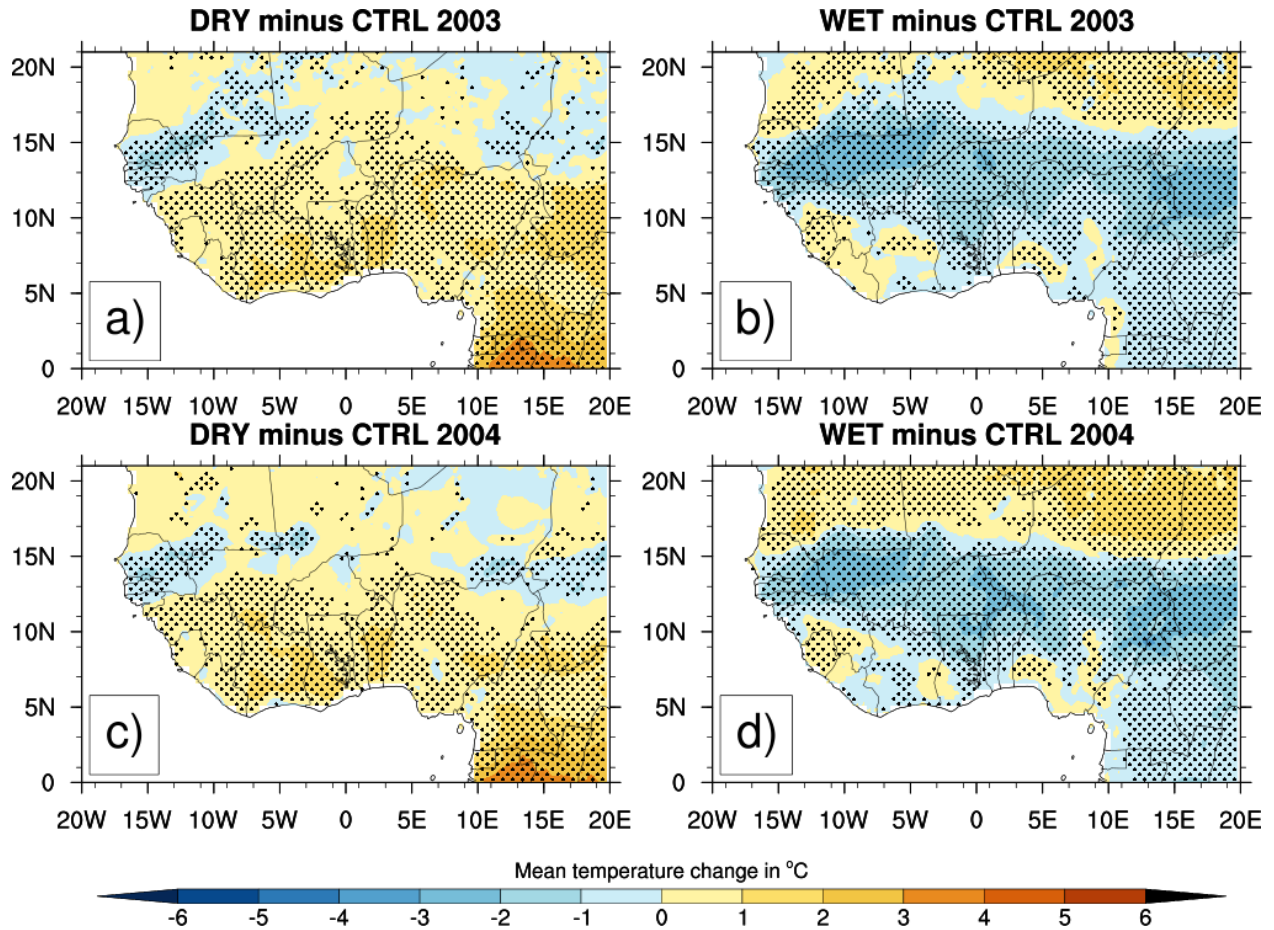


**Figure 12:** Changes in 2m-temperature (°C) for JJAS 2003 and JJAS 2004, from dry (resp. a and c) and wet (resp. b and d) experiments with respect to the control experiment, the dotted area shows differences that are statistically significant at 0.05 level.

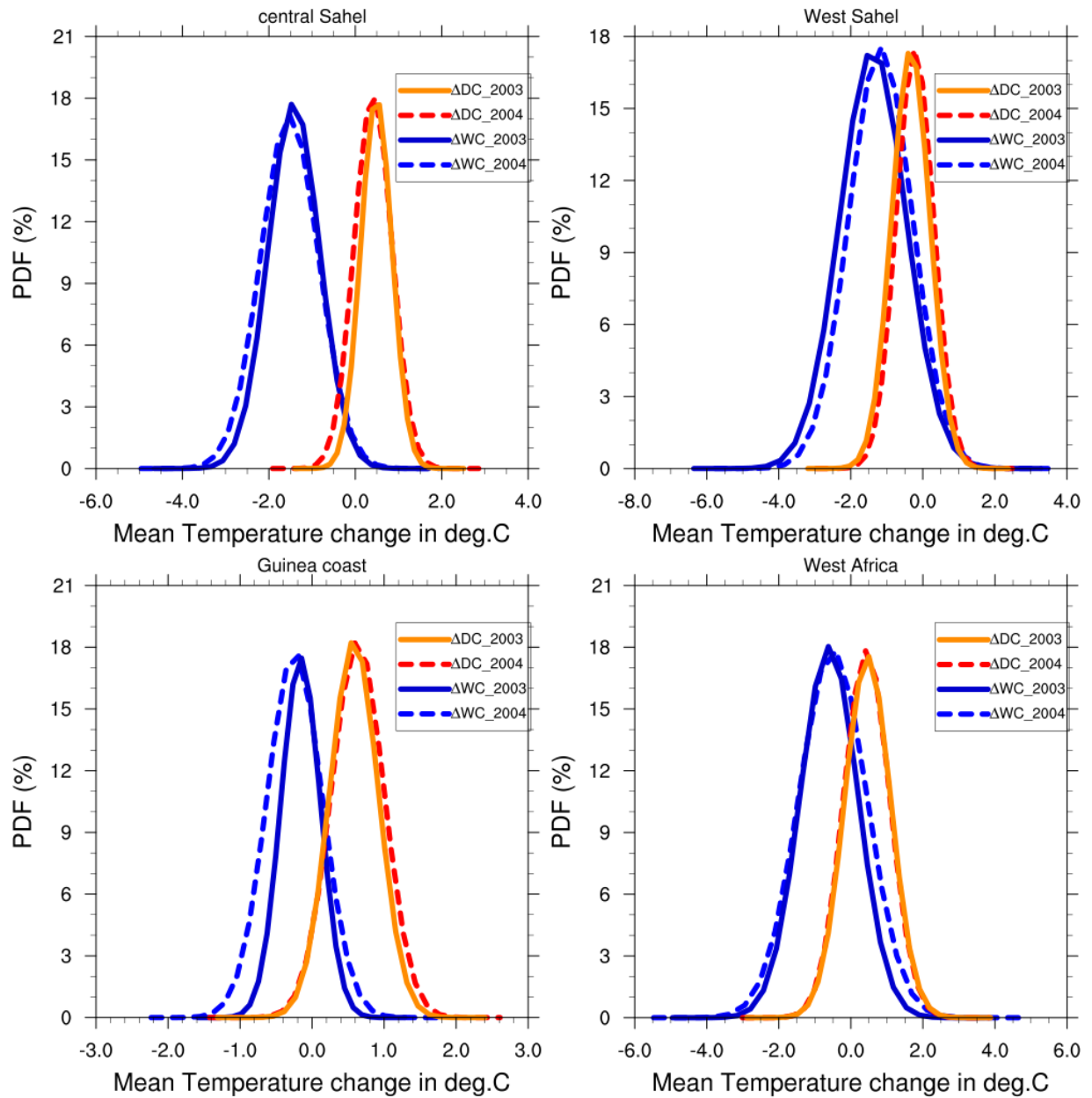


**Figure 13:** PDF distributions (%) of mean temperature changes in JJAS 2003 and JJAS 2004, over (a) central Sahel , (b) West Sahel, (c) Guinea and (d) West Africa derived from dry ( $\Delta DC$ ) and wet ( $\Delta WC$ ) experiments compared to the control experiment.



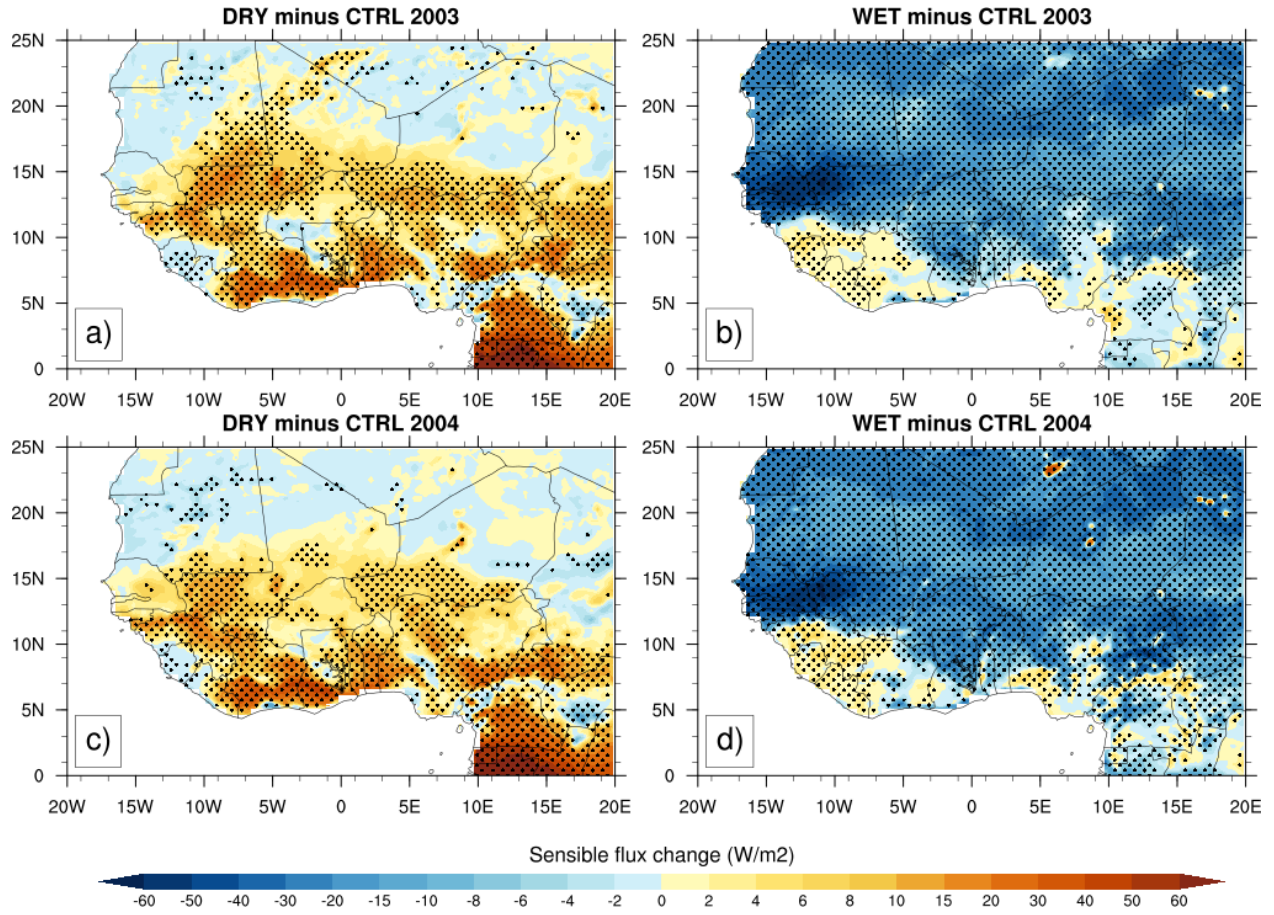


**Figure 14:** Same as Fig.12 but for sensible heat fluxes (in  $\text{W.m}^{-2}$ ).

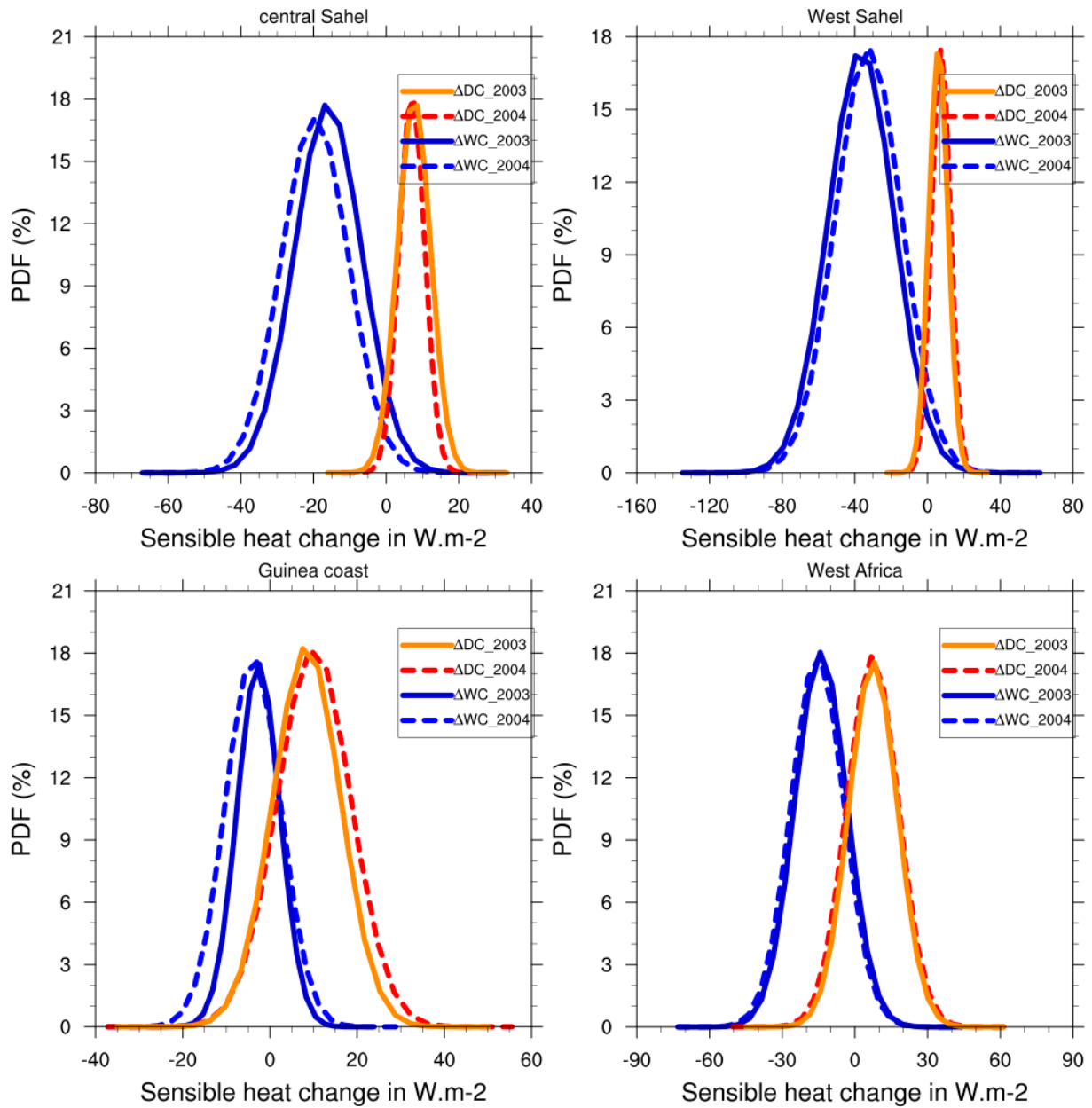


**Figure 15:** Same as Fig.13 but for sensible heat fluxes (in  $\text{W.m}^{-2}$ ).



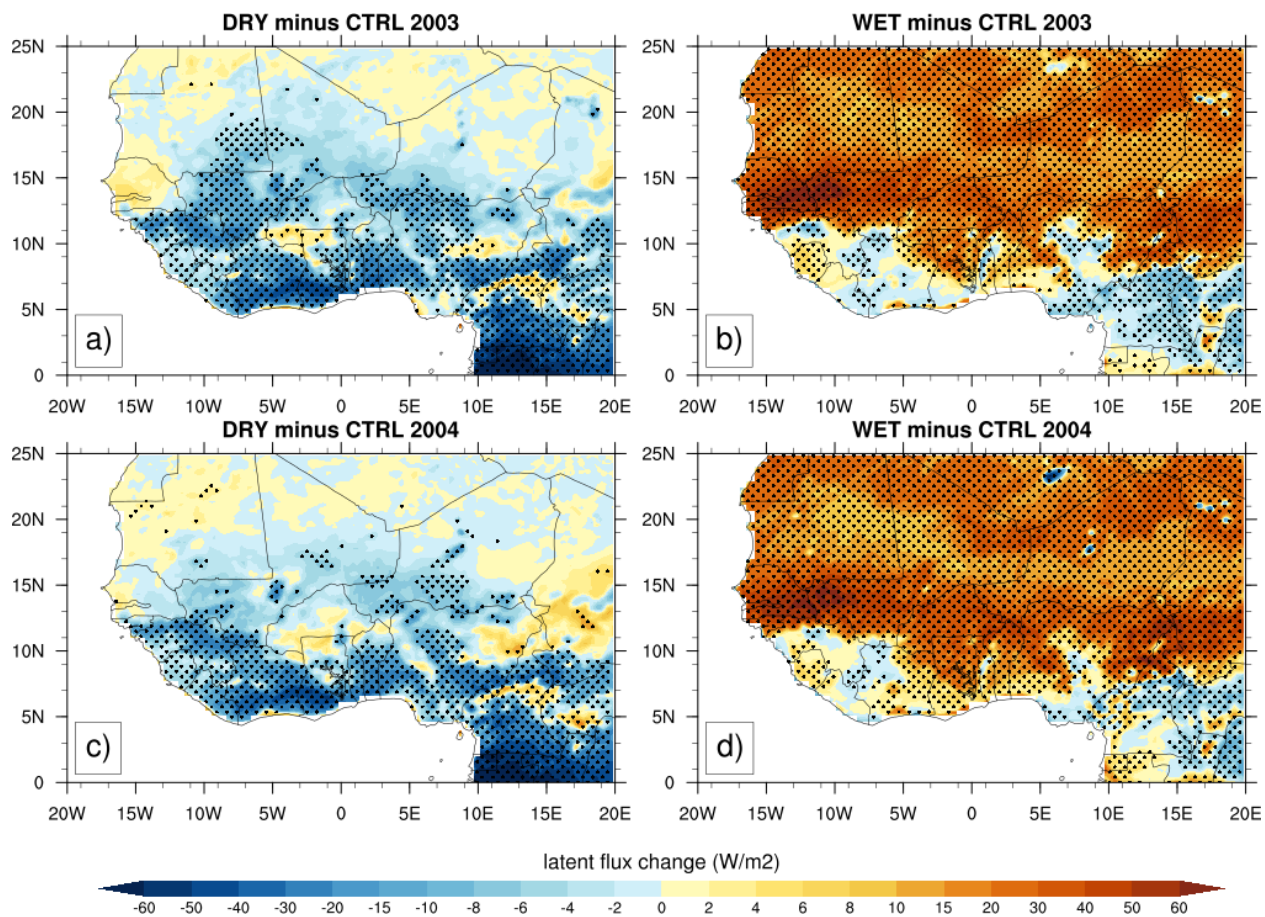


**Figure 16:** Same as Fig.12 but for latent heat fluxes (in  $\text{W.m}^{-2}$ ).

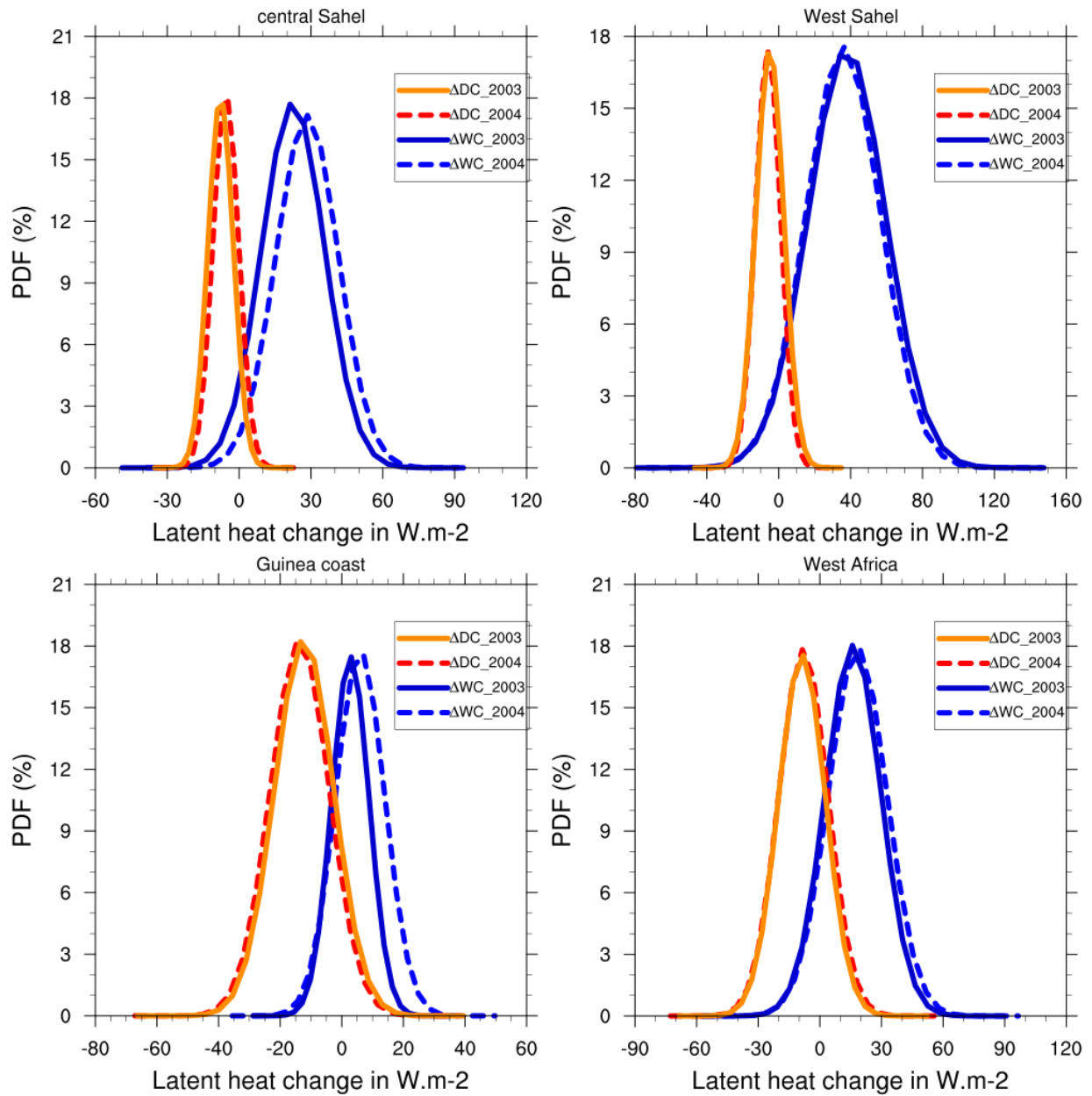


**Figure 17:** Same as Fig.13 but for latent heat fluxes (in  $\text{W.m}^{-2}$ ).

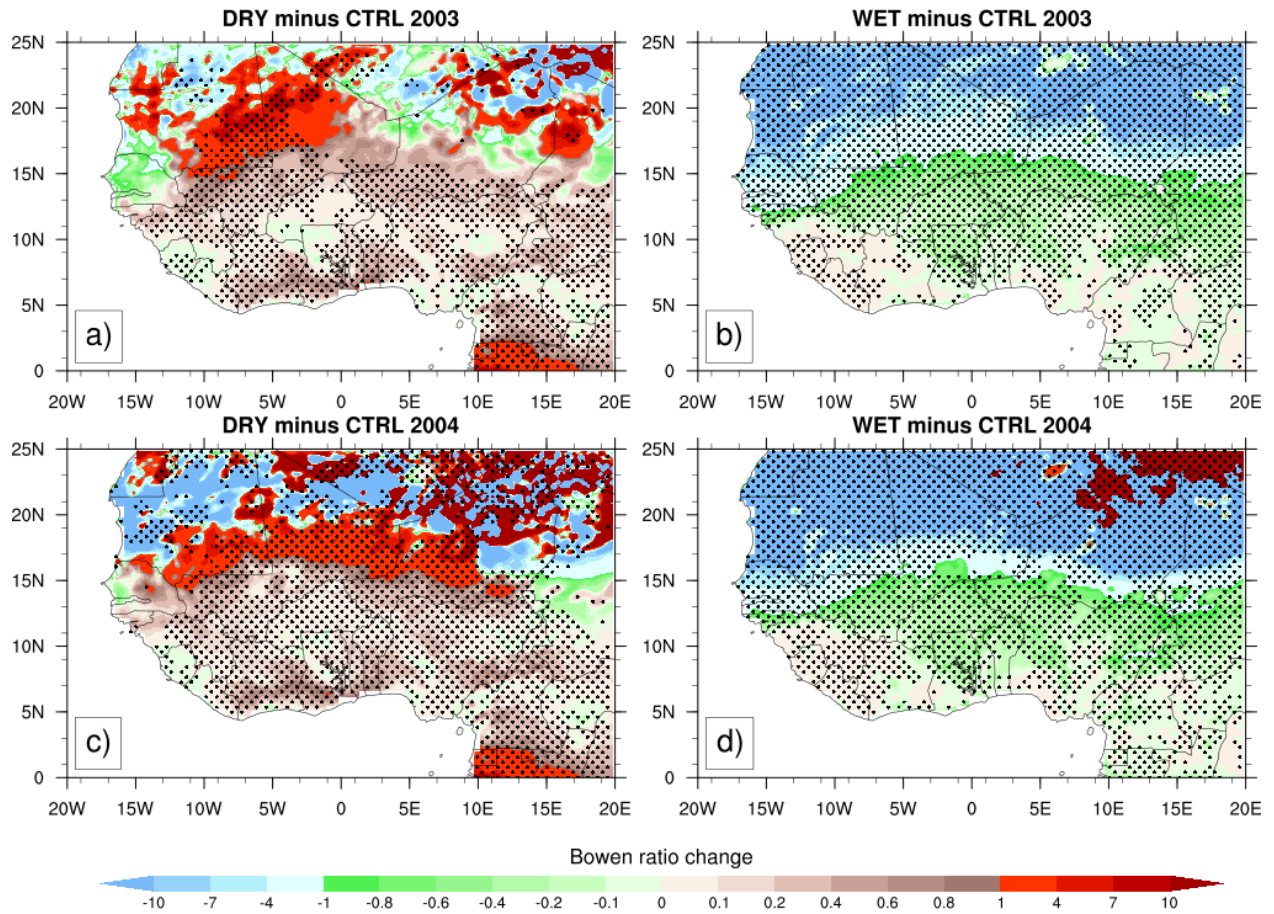


**Figure 18:** Same as Fig.12 but for Bowen ratio.

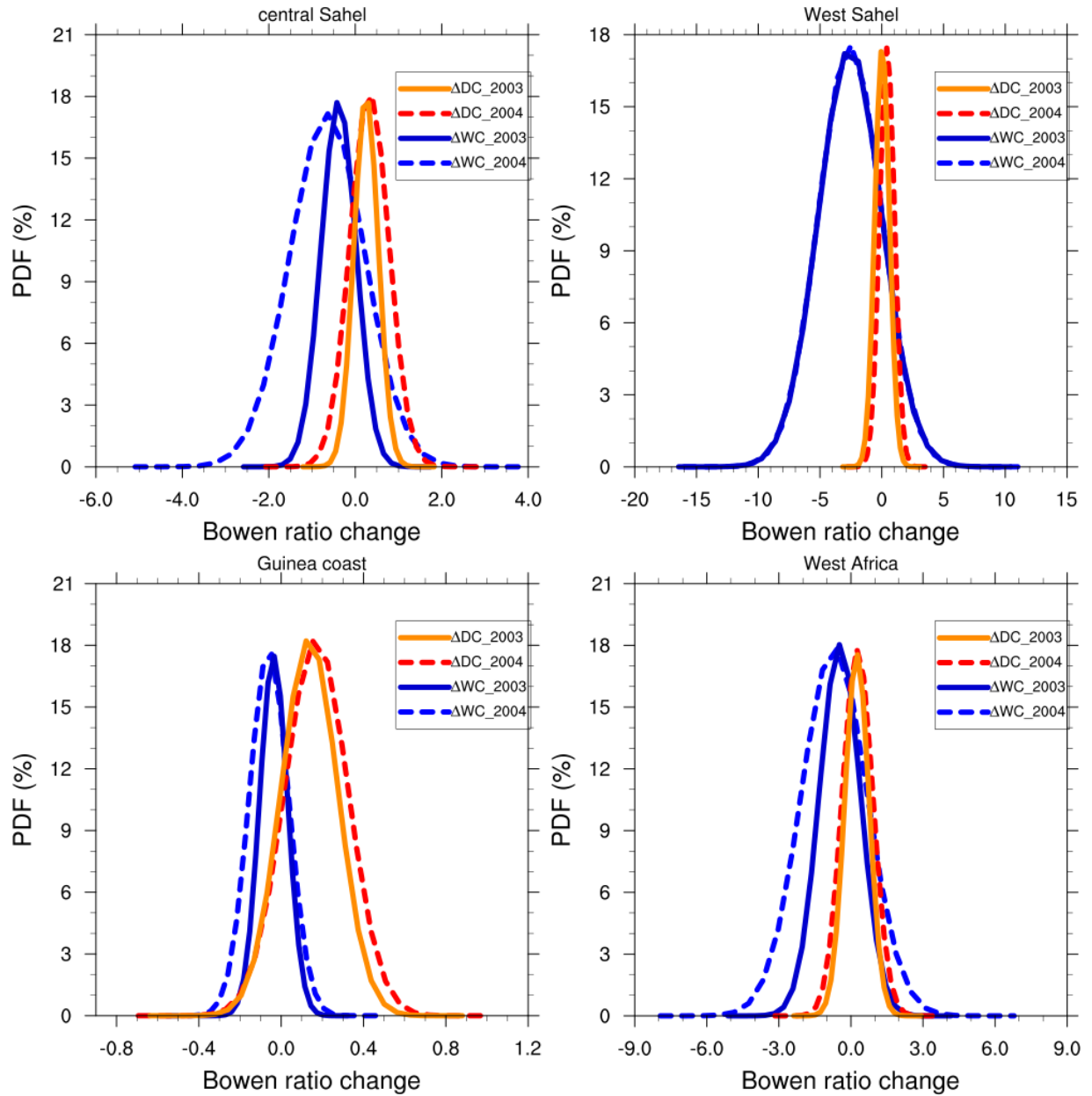


**Figure 19:** Same as Fig.13 but for Bowen ratio.

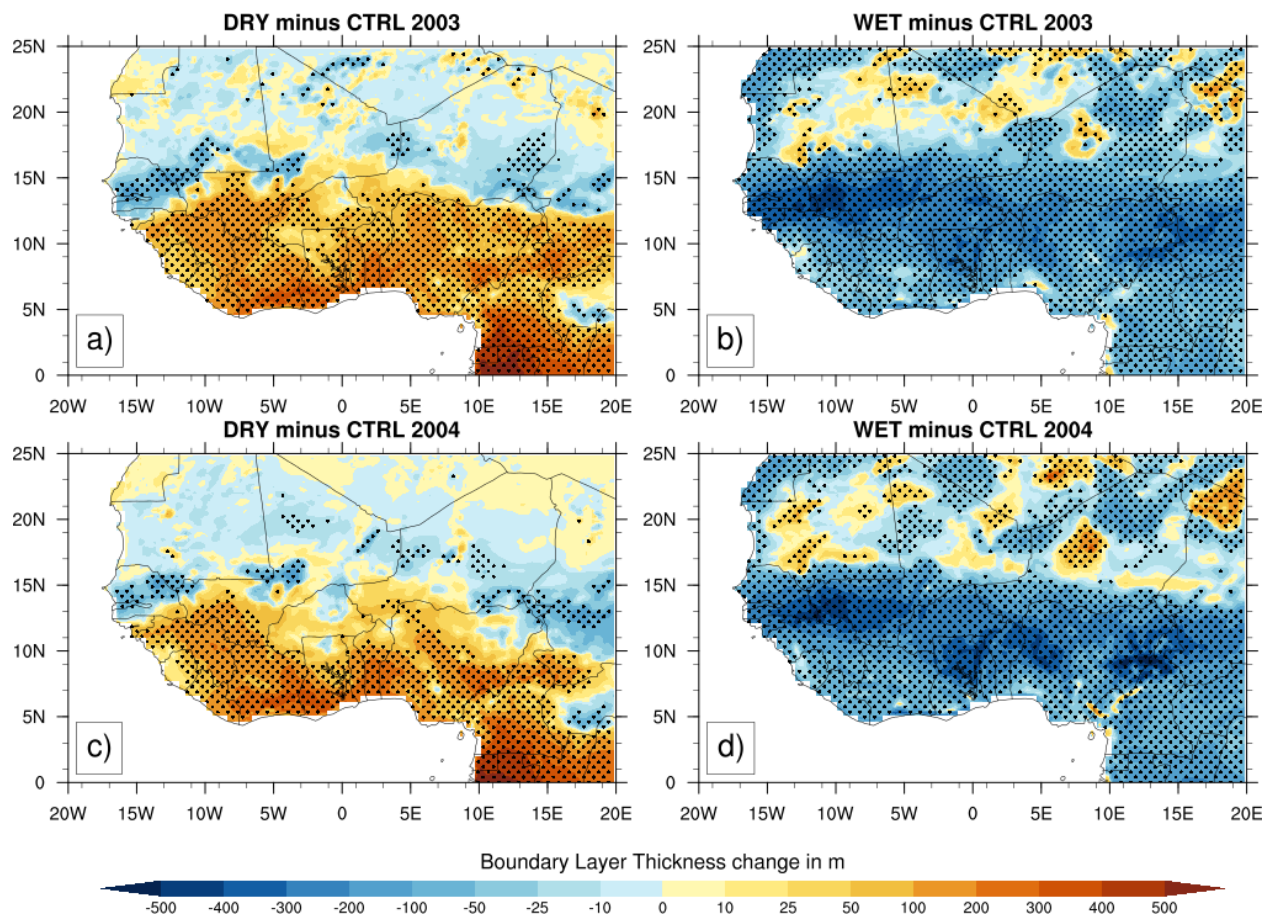


**Figure 20:** Same as Fig.12 but for the change of the height of the planetary boundary layer (in m).



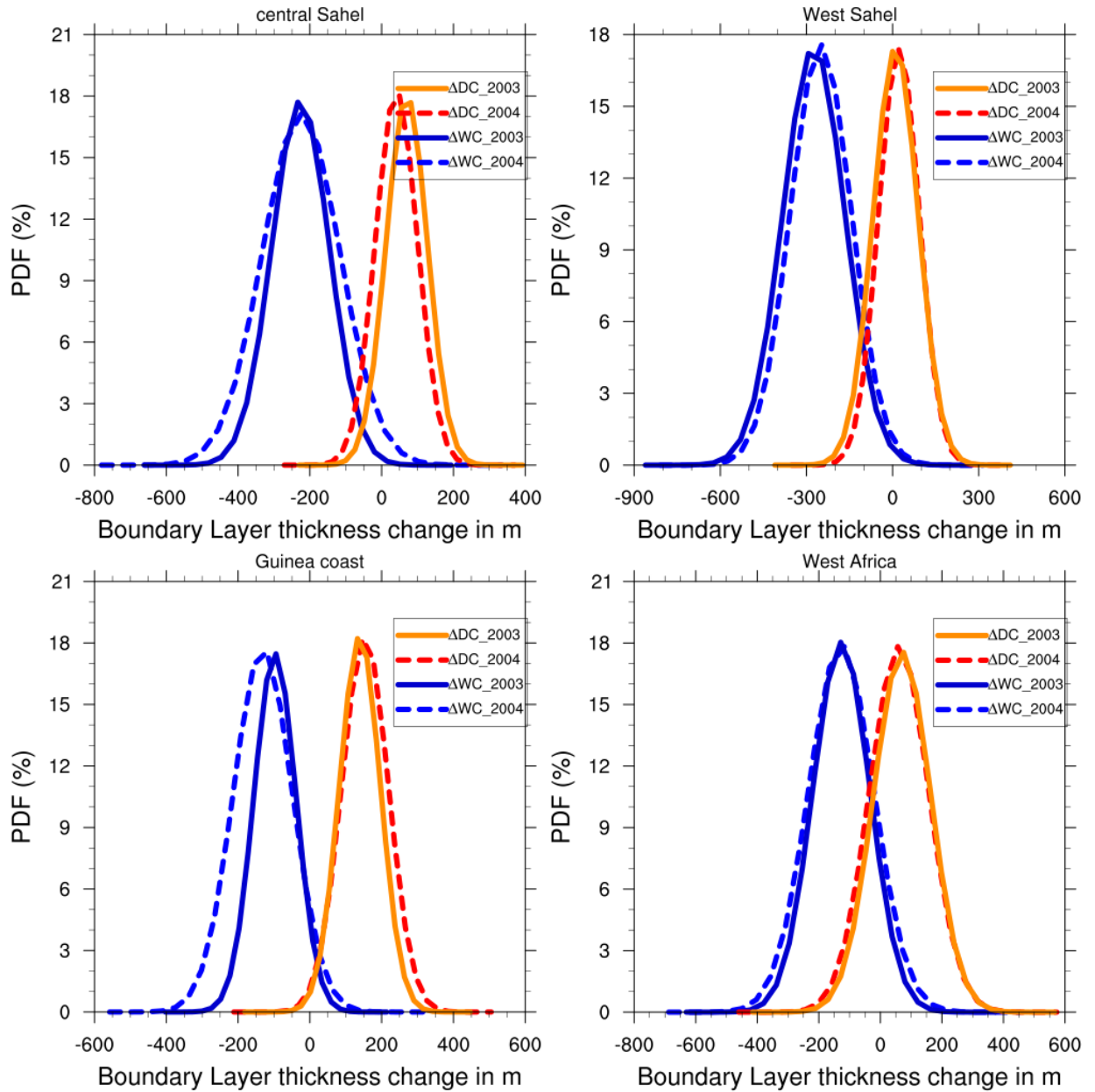


**Figure 21:** Same as Fig.13 but for the height of the planetary boundary layer (in m).

1060

1061

1062